# Design and synthesis of ibuprofen-quinoline conjugates as potential anti-inflammatory and analgesic drug candidates

Amany M. Ghanim[a,b], Adel S. Girgis[c], Benson M. Kariuki[d], Nermin Samir[e], Mona F. Said[f], Anwar Abdelnaser[g], Soad Nasr[g,h], Mohamed S. Bekheit[c], Mohamed F. Abdelhameed[i], Ahmad J. Almalki[j,k], Tarek S. Ibrahim[j], Siva S. Panda[a,*]

[a] *Department of Chemistry & Physics, Augusta University, Augusta, GA 30912, USA*
[b] *Department of Pharmaceutical Organic Chemistry Faculty of Pharmacy, Zagazig University, 44519 Zagazig, Egypt*
[c] *Department of Pesticide Chemistry, National Research Centre, Dokki, Giza 12622, Egypt*
[d] *School of Chemistry, Cardiff University, Main Building, Park Place, Cardiff CF10 3AT, UK*
[e] *Department of Pharmaceutical Chemistry, Faculty of Pharmacy, Ain Shams University, Cairo 11566, Egypt*
[f] *Department of Pharmaceutical Chemistry, Faculty of Pharmacy, Cairo University, Cairo 11562, Egypt*
[g] *Institute of Global Health and Human Ecology, School of Sciences and Engineering, The American University in Cairo (AUC), Cairo 11835, Egypt*
[h] *Institute of Pharmacology of Natural Products & Clinical Pharmacology, Ulm University, D-89081 Ulm, Germany*
[i] *Pharmacology Department, National Research Centre, Dokki, Giza 12622, Egypt*
[j] *Department of Pharmaceutical Chemistry, Faculty of Pharmacy, King Abdulaziz University, Jeddah 21589, Saudi Arabia*
[k] *Center of Excellence for Drug Research and Pharmaceutical Industries, King Abdulaziz University, Jeddah 21589, Saudi Arabia*

ARTICLE INFO

*Keywords:*
Ibuprofen
Quinoline
Anti-inflammatory
Analgesic
COX
QSAR

ABSTRACT

A new set of ibuprofen-quinoline conjugates comprising quinolinyl heterocycle and ibuprofen moieties linked by an alkyl chain were synthesized in good yields utilizing an optimized reaction procedure in a molecular hybridization approach to overcome the drawbacks of the current non-steroidal anti-inflammatory drugs. The synthesized conjugates were screened for their anti-inflammatory, and ulcerogenic properties. Several conjugates were found to have significant anti-inflammatory properties in the carrageenan-induced rat paw edema test without showing any ulcerogenic liability. In addition, most conjugates showed promising peripheral analgesic activity in the acetic acid-induced writhing test as well as central analgesic properties in the *in vivo* hot plate test. The most promising conjugates were the unsubstituted and 6-substituted fluoro- and chloro-derivatives of 2-(trifluoromethyl)quinoline linked to ibuprofen by a propyl chain. Their anti-inflammatory activity was evaluated against LPS-stimulated inflammatory reactions in RAW264.7 mouse macrophages. In this regard, it was found that most of the conjugates were able to significantly reduce the release and production of nitric oxide in the LPS-stimulated macrophages. The secretion and expression of the pro-inflammatory cytokines IL-6, TNF-α, and inducible nitric oxide synthase (iNOS) were also significantly suppressed.

## 1. Introduction

Non-steroidal anti-inflammatory drugs (NSAIDs) were introduced to the market in 1897 for the treatment of inflammation, pain, and fever. The utility of NSAIDs as analgesics and antipyretics is limited by their gastrointestinal side effects because of their non-selective inhibition towards COX-1 and COX-2, the two cyclooxygenase isoenzymes responsible for the conversion of arachidonic acid (AA) to prostaglandin $H_2$ ($PGH_2$) [1]. COX-1 plays a crucial role in cytoprotection in the stomach and intestine while COX-2 is expressed during inflammation. Although selective COX-2 inhibitors such as celecoxib and rofecoxib exhibit good anti-inflammatory activity without affecting the gastrointestinal tract, they are associated with high cardiovascular risks [2]. Because of these considerations, there is a need for innovative anti-inflammatory agents combining high efficacy along with an enhanced safety profile.

Ibuprofen (IBU), 2-(4-isobutylphenyl)propanoic acid, is one of the most extensively used NSAIDs in musculoskeletal disorders, osteoarthritis, and rheumatoid arthritis. In addition, it is the safest traditional choice for utilization during chronic neuroinflammation such as in

* Corresponding author.
*E-mail addresses:* sipanda@augusta.edu, sspanda12@gmail.com (S.S. Panda).

Parkinson's [3], Alzheimer's [4], and Machado-Joseph diseases [5]. Many routes have been described for masking the carboxylic acid functionality of ibuprofen including conversion to related esters [6] and amides [7] as well as conjugation with diverse drugs and heterocycles such as chloroxazone [8], menthol, thymol, eugenol [9] and quinazoline [10] to reduce gastric ulceration and improve its pharmacokinetic profile.

Additionally, quinoline-based derivatives **I**-**V** have aroused interest in the development of anti-inflammatory agents because of their high selectivity towards COX-2 rather than COX-1 Fig. 1 [11-15]. Notably, quinoline scaffolds exhibit inhibitory activity against inflammatory mediators such as lipoxygenase (15-LOX) [16], inducible nitric oxide synthase (iNOs) [17], toll-like receptor 4 (TLR4) [18], and hematopoietic prostaglandin D synthase (H-PGDS) [19].

In contrast to the known selective COX-2 inhibitors (e.g. coxibs), quinoline scaffolds exhibit cardioprotective properties *via* inhibition of cholesterol ester transfer protein (CETP), a key risk factor for cardiovascular diseases such as low HDL-C and atherosclerosis [20]. Also, many quinoline derivatives are reported to have excellent agonist potency towards liver X receptors (LXRa and LXRb) [21,22] and bradykinin BK $B_2$ receptor [23] displaying a therapeutic potential in the regulation of cholesterol and lipid metabolism.

Our recent attempt to synthesize IBU-hybrid conjugates with the bioactive acetaminophen through amino acid linkers developed mutual prodrugs (**VI** and **VII**) that exhibit effective analgesic activity with no ulcerogenic liability Fig. 2 [24,25]. Encouraged by these results, the present study describes the design and synthesis of novel IBU-quinoline hybrid conjugates by tethering these two pharmacophores with saturated carbon chains of different lengths Fig. 3**.** The synthesized hybrids were screened for their anti-inflammatory, and ulcerogenic properties. Furthermore, the observed biological data were validated by computational studies.

Macrophages are the primary line of defense against infections [26]. Macrophages are activated *via* toll-like receptors (TLRs) signaling pathways. TLR4 ligates with lipopolysaccharide (LPS) which acts as a signal activator leading to the induction of intracellular pathways [27,28]. As a result, these intracellular pathways induce expression of inflammatory mediators exemplified by the pro-inflammatory cytokines such as interleukin-6 (IL-6) and tumor necrosis factor-α (TNF-*α*) in addition to inducible nitric oxide synthase (iNOS). Therefore, it has been shown that active ingredients with the ability to reduce LPS-stimulated inflammatory mediators can be used as anti-inflammatory therapeutic agents [29]. In the current study, the results support the anti-inflammatory effect of the target ibuprofen conjugates in LPS-stimulated murine RAW264.7 macrophages.

## 2. Results and discussion

### 2.1. Chemistry

The synthetic pathways employed to afford the novel ibuprofen-quinoline conjugates **8** and **9** are depicted in Schemes 1-3. First, the synthesis of 6-substituted-2-(trifluoromethyl)quinoline-4(1*H*)-ones **3a-d** was performed using Conrad-Limpach cyclocondensation [30]. The quinolones obtained were alkylated using dibromoalkanes (x, y, and z) in the presence of $K_2CO_3$ [31,32]. This step resulted in a mixture of the major *O*-alkylated quinolines **4**, and the minor *N*-alkylated quinolones **5** and bis-derivatives **6** as illustrated in Scheme 1. All the compounds in the mixture were separated by column chromatography and identified by spectroscopic studies. In addition, two of the *O*-alkylated quinolones (**4dz** and **4cx**) we confirmed by X-ray studies (Fig. 4).

A microwave-assisted *O*-alkylation of the free carboxylic acid moiety in ibuprofen **7** was achieved with 4-(bromoalkoxy)-2-(trifluoromethyl) quinolines **4** and 1-(bromoalkyl)-2-(trifluoromethyl)quinoline-4(1*H*)-ones **5az, 5dz** (Scheme 2 and Scheme 3) to provide the target ibuprofen-quinoline conjugates **8** and **9** respectively. The structures of the synthesized compounds were fully characterized and confirmed by spectroscopic studies.

### 2.2. Crystal structure determination

Crystals suitable for X-ray single-crystal structure determination were obtained for intermediates **4dz** and **4cx**. The molecular structure of **4dz** is shown in Fig. 4a. In the crystal structure, the bromo-hexyl chain assumes an all-trans conformation with C- C- C- C/Br torsion angles deviating no more than 1.7° from the ideal angle of 180°. The least-squares planes through the bromohexyl chain and the oxymethylquinoline group are co-planar with a twist angle of only 1.89 (31)°. The chain geometry and the relationship between the two planar groups are akin to that observed for 4-alkoxypyridines [33]. The molecular structure of **4cx** is shown in Fig. 4b. In the crystal structure, the bromopropyl group takes gauche conformation with torsion angles C11-C12-C13-Br1 and O1-C11-C12-C13 of 61.5(5)◦ and 59.7(6)◦ respectively, whereas the C12-C11-O1-C4 bond is trans with an angle of 176.6(4)◦.

### 2.3. Anti-inflammatory properties

The standard technique (carrageenan-induced rat paw edema) was utilized for the anti-inflammatory testing of the synthesized ibuprofen-quinoline conjugates **8** [25,34]. The results are presented in Table 1

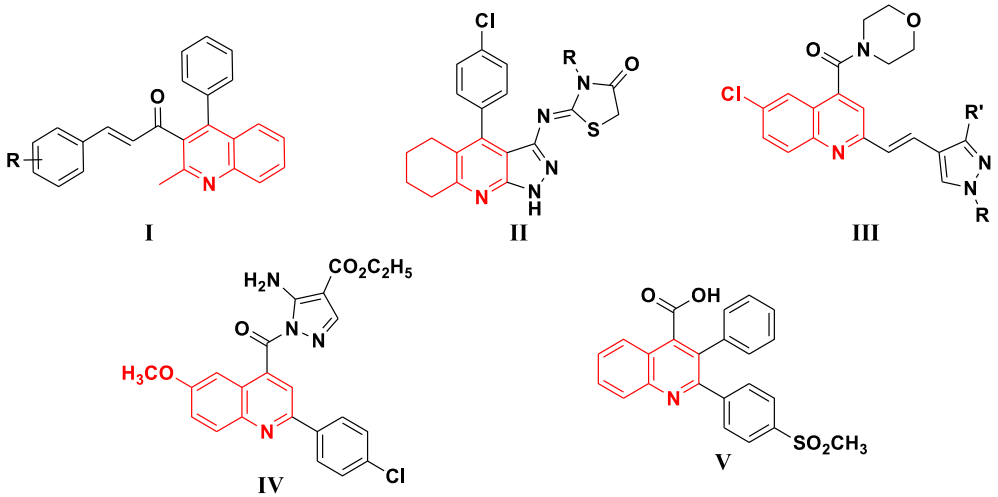


**Fig. 1.** Chemical structures of some reported quinoline-based selective COX-2 inhibitors (**I-V**).

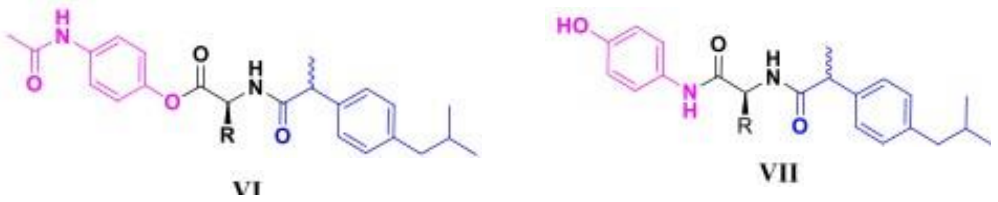


**Fig. 2.** Amino acid-linked IBU acetaminophen anti-inflammatory agents.

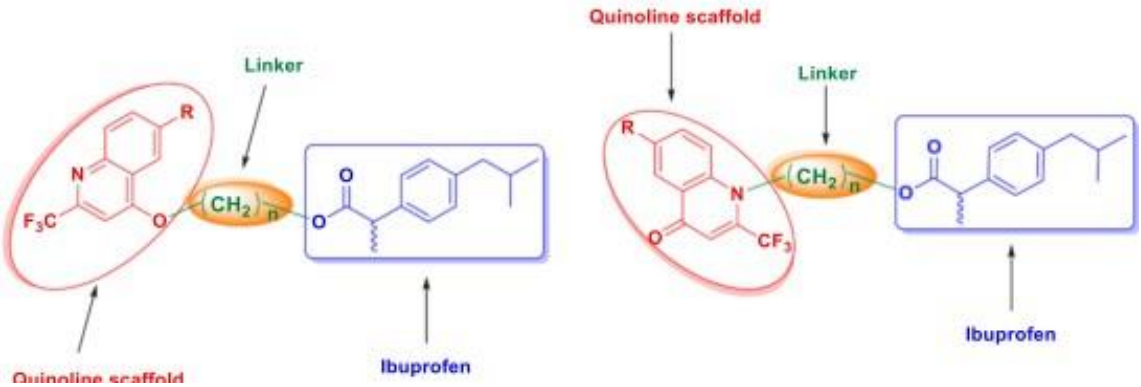


**Fig. 3.** The target IBU-quinoline conjugates.

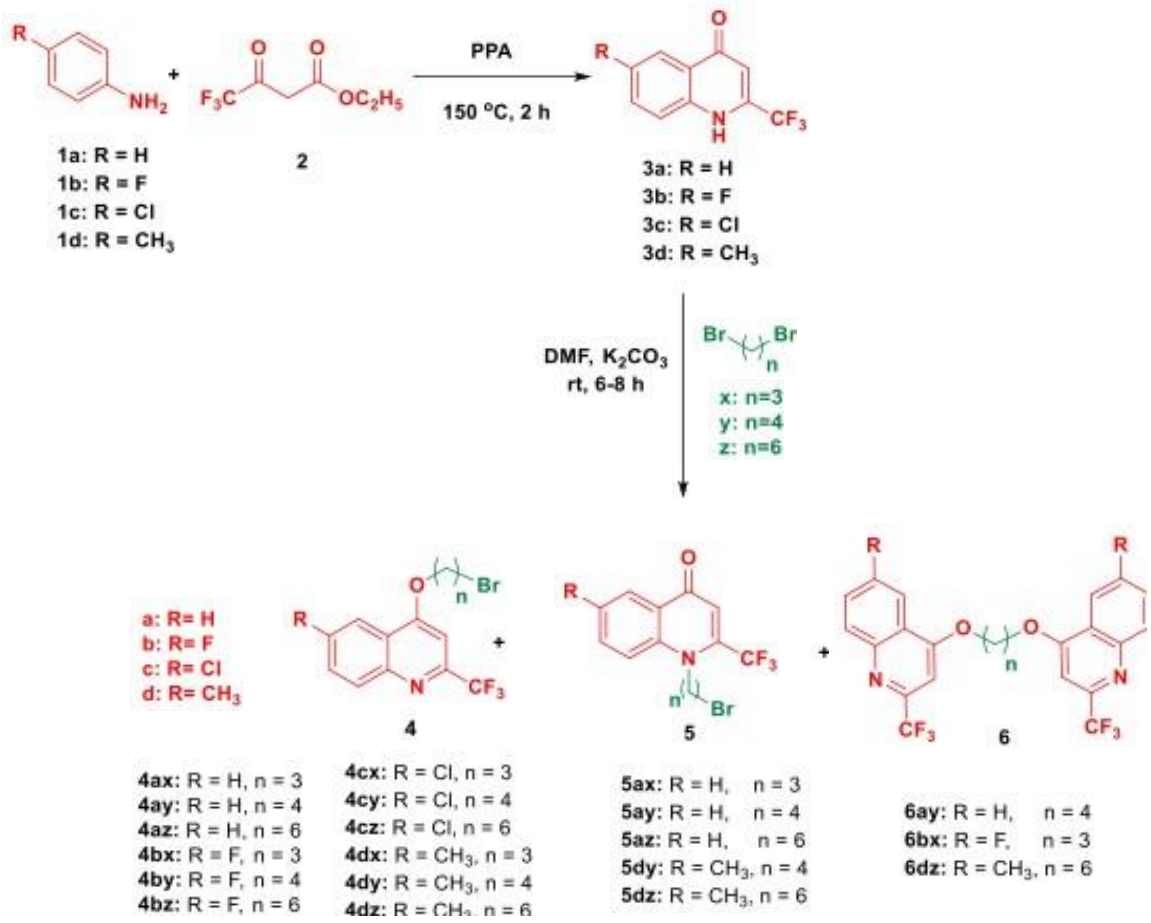


**Scheme 1.** Synthesis of 6-substituted-2-(trifluoromethyl)quinoline derivatives **4**, **5** and **6**.

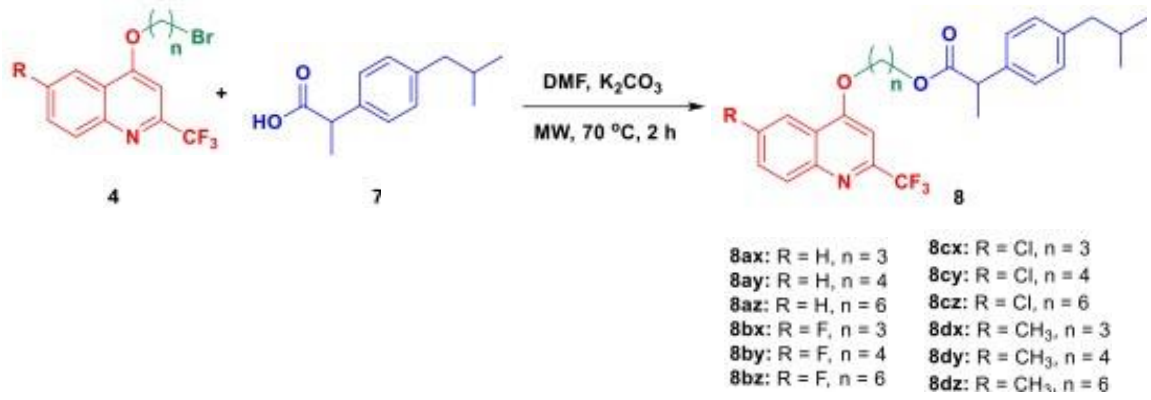


**Scheme 2.** Synthesis of conjugates **8**.


**Scheme 3.** Synthesis of conjugates **9az** and **9dz**.

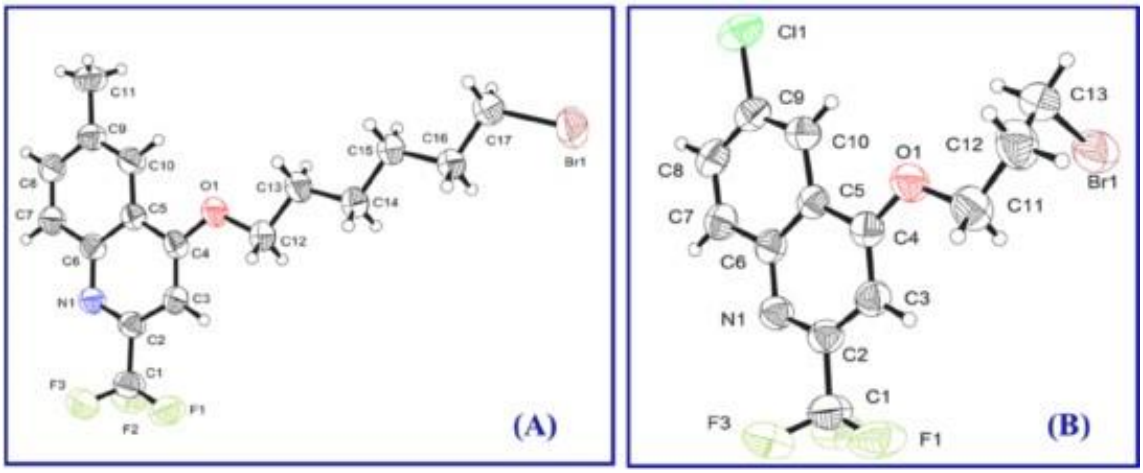


**Fig. 4.** Ortep representation of compounds (a) **4dz** and (b) **4cx** showing 50% probability displacement ellipsoids for non-H atoms.

and Fig. 5. Some of the analogs (**8ax, 8cx,** and **8bx**) show promising anti-inflammatory properties comparable to their precursor at 3 h (ibuprofen, which is a clinically approved anti-inflammatory drug revealing its maximum anti-inflammatory activity at 3 h). Their potencies = 96.2%, 96.7%, and 105.1% respectively, relative to indomethacin compare favorably with the anti-inflammatory properties of ibuprofen which has a value of 97.4%. It is notable that the edema volume in the control group is almost stable (mean edema thickness) throughout all the experimental time intervals (1-4 h) and it dropped at 24 h. It is observed that **8ax, 8cx,** and **8bx** show weak (at 1 h) and mild (at 2 h) anti-inflammatory activity, however; the potencies are elevated by time (at 3 h and 4 h) revealing their promising activity at 3 h relative to the standard drugs used. Therefore, they were considered promising agents.

Some SAR (structure-activity relationships) are observed. The substituent of the quinolinyl heterocycle seems to be a factor in the revealed bio-properties. The fluorine substituent has superior properties compared to chlorine and methyl as illustrated by compounds **8by/8cy/8dy, 8bx/8cx/8dx,** and **8bz/8cz/8dz.**

The length of the alkyl chain connecting ibuprofen and quinolinyl heterocycle also plays a role in controlling bioactivity. The three-carbon atom chain seems to be more suitable for developing enhanced anti-inflammatory agents than the four and six atom chains as shown by compounds **8bx**/**8by**/**8bz**, **8ax**/**8ay**/**az**, **8cx**/**8cy**/**8cz,** and **8dx**/**8dy**/**8dx**.

### *2.4. Analgesic properties*

#### *2.4.1. Peripheral analgesic testing*

Peripheral analgesic testing of the synthesized ibuprofen conjugates was conducted by the standard technique in mice (acetic acid-induced abdominal writhing) [25,34]. Table 2 (Fig. 6) shows the results observed which are exhibited in terms of % inhibition/protection and % potency of the compounds relative to indomethacin (drug/standard

**Table 1**
Anti-inflammatory properties at 10 mg kg[1] (rat body weight) indomethacin mol equivalent.

| Entry | Compd. | Mean edema thickness "mm" (% inhibition of edema ± SE "standard error") | | | | | % Potency[a] |
|---|---|---|---|---|---|---|---|
| | | 1 h | 2 h | 3 h | 4 h | 24 h | |
| 1 | Control | 0.837 ± 0.05 (0.00 ± 0.02) | 0.873 ± 0.01 (0.00 ± 0.01) | 0.823 ± 0.07 (0.00 ± 0.03) | 0.823 ± 0.09 (0.00 ± 0.00) | 0.397 ± 0.08 (0.00 ± 0.06) | — |
| 2 | Indo[b] | 0.495 ± 0.02** (40.9 ± 1.3) | 0.432 ± 0.06** (50.5 ± 1.6) | 0.156 ± 0.03** (81.0 ± 1.9) | 0.404 ± 0.04** (50.9 ± 2.2) | 0.343 ± 0.01** (13.6 ± 1.3) | 100 |
| 3 | IBU | 0.465 ± 0.03** (44.4 ± 1.1) | 0.493 ± 0.06** (43.5 ± 1.8) | 0.174 ± 0.07** (78.9 ± 2.3) | 0.650 ± 0.11** (21.0 ± 1.5) | 0.351 ± 0.06** (11.6 ± 1.9) | 97.4 |
| 4 | **8ax** | 0.770 ± 0.01* (8.0 ± 0.4) | 0.663 ± 0.08** (24.1 ± 1.3) | 0.182 ± 0.03** (77.9 ± 1.9) | 0.147 ± 0.06** (82.1 ± 2.1) | 0.197 ± 0.01** (50.4 ± 1.8) | 96.2 |
| 5 | **8ay** | 0.400 ± 0.08** (52.2 ± 1.5) | 0.520 ± 0.04** (40.4 ± 1.9) | 0.510 ± 0.01** (38.0 ± 1.1) | 0.507 ± 0.09** (38.4 ± 2.4) | 0.370 ± 0.06* (6.8 ± 0.4) | 46.9 |
| 6 | **8az** | 0.787 ± 0.05* (6.0 ± 0.8) | 0.563 ± 0.01** (35.5 ± 2.0) | 0.510 ± 0.04** (38.0 ± 1.4) | 0.503 ± 0.05** (38.9 ± 2.3) | 0.273 ± 0.02** (31.2 ± 1.1) | 46.9 |
| 7 | **8bx** | 0.813 ± 0.06** (2.9 ± 0.03) | 0.643 ± 0.02** (26.3 ± 1.5) | 0.123 ± 0.07** (85.1 ± 2.8) | 0.077 ± 0.01** (90.6 ± 1.1) | 0.360 ± 0.03* (9.3 ± 0.9) | 105.1 |
| 8 | **8by** | 0.617 ± 0.08** (26.3 ± 1.7) | 0.600 ± 0.09** (31.3 ± 0.3) | 0.433 ± 0.05** (47.4 ± 2.5) | 0.137 ± 0.05** (83.4 ± 3.0) | 0.290 ± 0.01** (27.0 ± 2.2) | 58.5 |
| 9 | **8bz** | 0.527 ± 0.09** (37.0 ± 2.1) | 0.427 ± 0.01** (51.1 ± 1.6) | 0.453 ± 0.08** (45.0 ± 1.6) | 0.393 ± 0.06** (52.2 ± 2.3) | 0.100 ± 0.04** (74.8 ± 2.9) | 55.6 |
| 10 | **8cx** | 0.790 ± 0.01* (5.6 ± 0.5) | 0.604 ± 0.09** (30.8 ± 2.1) | 0.179 ± 0.09** (78.3 ± 1.3) | 0.275 ± 0.01** (66.6 ± 0.07) | 0.376 ± 0.05** (5.3 ± 1.1) | 96.7 |
| 11 | **8cy** | 0.661 ± 0.07** (21.0 ± 2.1) | 0.636 ± 0.08** (27.1 ± 1.9) | 0.478 ± 0.04** (41.9 ± 2.4) | 0.464 ± 0.09** (43.6 ± 2.7) | 0.179 ± 0.08** (54.9 ± 2.2) | 51.7 |
| 12 | **8cz** | 0.576 ± 0.06** (31.2 ± 1.1) | 0.337 ± 0.02** (61.4 ± 1.6) | 0.481 ± 0.06** (41.6 ± 1.4) | 0.603 ± 0.02** (26.7 ± 1.2) | 0.321 ± 0.05* (19.1 ± 2.4) | 51.4 |
| 13 | **8dx** | 0.788 ± 0.07* (5.9 ± 0.9) | 0.453 ± 0.09** (48.1 ± 2.3) | 0.546 ± 0.06** (33.7 ± 2.0) | 0.620 ± 0.08** (24.7 ± 1.9) | 0.057 ± 0.06** (85.6 ± 2.7) | 41.6 |
| 14 | **8dy** | 0.501** ± 0.06 (40.1 ± 2.3) | 0.353 ± 0.09** (59.6 ± 1.8) | 0.557 ± 0.08** (32.3 ± 2.2) | 0.664 ± 0.07** (19.3 ± 2.1) | 0.273 ± 0.09** (31.2 ± 2.6) | 39.9 |
| 15 | **8dz** | 0.744 ± 0.09* (11.1 ± 1.9) | 0.517 ± 0.06** (40.8 ± 1.5) | 0.708 ± 0.03* (14.0 ± 0.9) | 0.813 ± 0.01* (1.2 ± 0.3) | 0.387 ± 0.08* (2.5 ± 0.7) | 17.3 |

Statistical analysis was carried out by one-way ANOVA *$p < 0.05$, **$p < 0.001$.
[a] Potency is the % inhibition of the edema thickness compared to indomethacin at 3 h. [b] Indo is indomethacin.

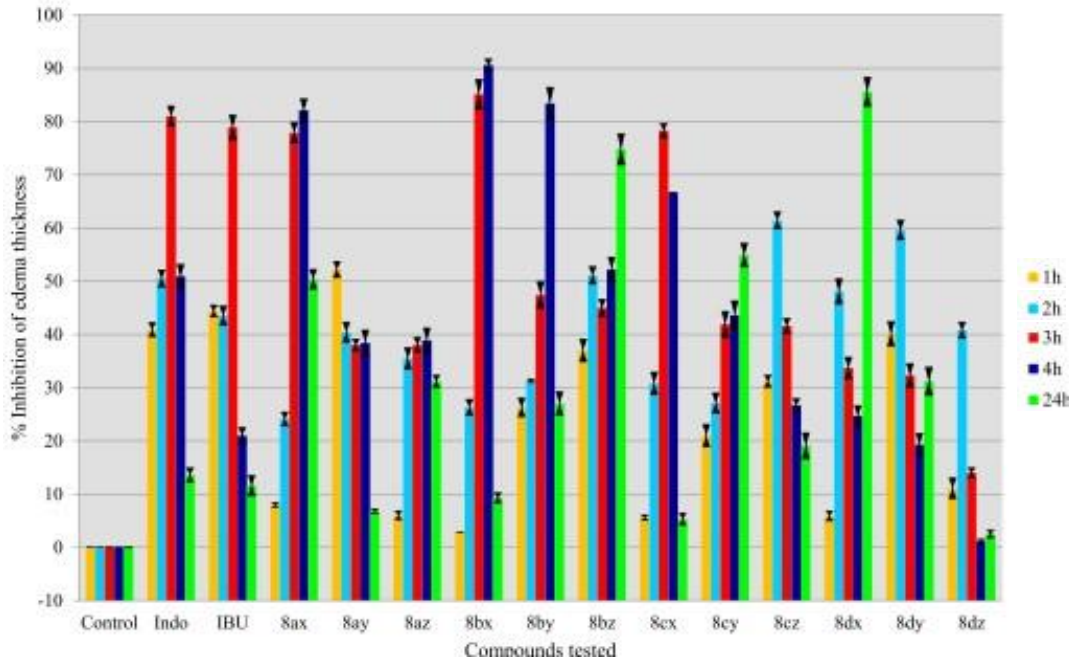


**Fig. 5.** % Inhibition of edema thickness by the tested compounds.

reference). All the synthesized conjugates show enhanced peripheral analgesic properties relative to their precursor/parent drug (ibuprofen). Additionally, all the synthesized agents (**8dy** is an exception) reveal better peripheral analgesic properties in comparison to that of indomethacin. Notably, indomethacin exhibits higher peripheral analgesic properties than ibuprofen (% protection is 71.8 for indomethacin and 58.5 for ibuprofen). Compounds **8bz**, **8cx**, **8cz,** and **9az** are the most effective of the agents synthesized with the highest potency relative to indomethacin (% potency = 136.9-138.6).

A number of SARs are evident based on the results obtained. The

**Table 2**
Peripheral analgesic properties at 10 mg kg[1] (mice body weight) indomethacin mol equivalent.

| Entry | Compd. | Writing reflex ± SE | % Inhibition/ protection | % Potency[a] |
|---|---|---|---|---|
| 1 | Control | 40 ± 3.2 | 0 | — |
| 2 | Indomethacin | 11.3 ± 1.6** | 71.8 | 100.0 |
| 3 | IBU | 16.6 ± 0.7** | 58.5 | 81.5 |
| 4 | **8ax** | 4.5 ± 0.1* | 88.8 | 123.7 |
| 5 | **8ay** | 10.7 ± 0.9* | 73.3 | 102.1 |
| 6 | **8az** | 1.3 ± 0.1** | 96.8 | 134.8 |
| 7 | **8bx** | 1.3 ± 0.09** | 96.8 | 134.8 |
| 8 | **8by** | 10.5 ± 0.8* | 73.8 | 102.8 |
| 9 | **8bz** | 0.3 ± 0.02** | 99.3 | 138.3 |
| 10 | **8cx** | 0.7 ± 0.04** | 98.3 | 136.9 |
| 11 | **8cy** | 3.7 ± 0.3** | 90.8 | 126.5 |
| 12 | **8cz** | 0.2 ± 0.01** | 99.5 | 138.6 |
| 13 | **8dx** | 6.3 ± 0.4** | 84.3 | 117.4 |
| 14 | **8dy** | 11.9 ± 0.8* | 70.3 | 97.9 |
| 15 | **8dz** | 1.7 ± 0.03** | 95.8 | 133.4 |
| 16 | **9az** | 0.7 ± 0.01** | 98.3 | 136.9 |
| 17 | **9dz** | 7.7 ± 0.7** | 80.8 | 112.5 |

Statistical analysis was carried out by one-way ANOVA *$p < 0.05$, **$p < 0.001$.
[a] Potency is the % inhibition/protection relative to indomethacin.

substituent of the quinolinyl heterocycle seems to influence the bio-properties. The halogen-substituted quinolinyl conjugate has enhanced peripheral analgesic properties relative to the unsubstituted or methyl-substituted group (as exhibited by compounds **8by/8cy/8ay/8dy, 8bx/8cx/8ax/8dx,** and **8bz/8cz/8az/8dz**). Additionally, chloro-substituted quinolinyl conjugates are more effective peripheral analgesic agents than the fluoro-containing analogs (as exhibited in pairs **8bx**/**8cx**, **8by**/**8cy,** and **8bz**/**8cz**). The length of the alkyl chain linking the quinolinyl heterocycle with ibuprofen also influences the analgesic properties observed. The six-carbon linker (hexyl) is more suitable than the four and three carbon linkers (butyl and propyl).

### 2.4.2. Central analgesic testing

The hot plate standard technique in mice was utilized for central analgesic testing of the synthesized agents [25,34]. From the data (Table 3, Fig. 6), it is clear that only compounds **8ay** and **9az** show potency close to their parent drug (potency is 94.3% for **8ay**, 92.6% for **9az,** and 96.1% for ibuprofen). It is also notable that compound **8az** reveals higher central analgesic properties after the first 30 min. time interval relative to the standard references (% protection = 99.0, 87.1, 61.7 for **8az**, indomethacin, and ibuprofen, respectively). The biological properties are drastically reduced over time (% protection = 18.2, 56.5, 54.3 for **8az**, indomethacin, and ibuprofen, respectively at 120 min.). The same observations are also made for compounds **8by**, **8dx,** and **8cx** (% protection = 97.2, 93.1, 89.1 respectively at 30 min. and 32.0, 47.2, 7.5 respectively at 120 min.).

Some SARs are notable from the revealed biological properties. The length of the alkyl chain linking the quinolinyl heterocycle and ibuprofen is important in controlling the bio-properties. The butyl-linker-containing compounds show higher biological activity than the propyl linker-possessing analogs. The latter in turn reveals higher bio-properties than the hexyl linker-containing conjugates (as shown by the central analgesic properties of compounds **8by>8bx>8bz**, **8ay>8ax>8az**, **8cy>8cx>8cz,** and **8dy>8dx>8dz**). Additionally, the methyl-substituted quinolinyl-containing conjugates have better higher biological properties than the halogenated quinolinyl analogs as shown by compounds **8dy/8by/8cy, 8dx/8bx/8cx,** and **8dz/8bz/8cz** Moreover, the fluoroquinolinyl conjugates have higher biological activities than the chloroquinolinyl compounds, as shown in pairs **8by**/**8cy**, **8bx**/**8cx** and **8bz**/**8cz** (% protection = 56.6, 28.1; 55.6, 13.3; 34.3, 13.1 for **8by**, **8cy**; **8bx**, **8cx,** and **8bz**, **8cz** respectively)

### 2.5. Ulcerogenic liability

Ulcerogenic liability testing for the most promising anti-inflammatory active agents synthesized (**8ax, 8bx**, and **8cx**) in addition to the reference standard (indomethacin and ibuprofen) was performed utilizing the standard technique in mice [25,34]. Table 4 reveals that compound **8ax** shows ulcers but with milder severity relative to its parent drug (ulcer index = 2.01, 4.33 for **8ax** and ibuprofen, respectively). However, no ulcers or erosions to the tested animal gastric mucosa were observed for the other two anti-inflammatory active agents tested (**8bx** and **8cx**) revealing their safe applicability for oral administration.

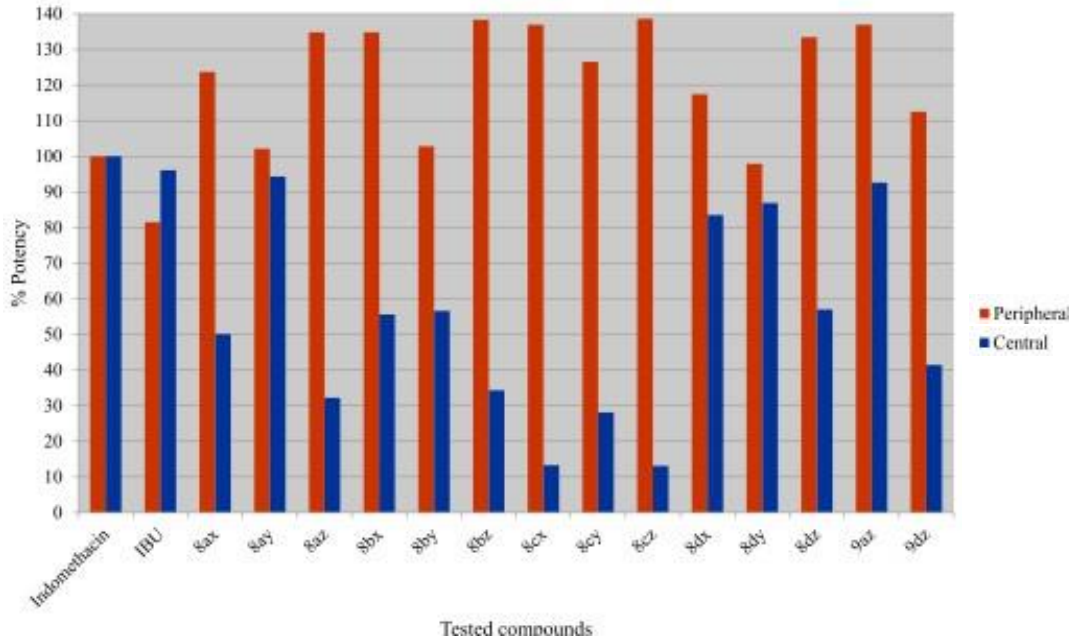


**Fig. 6.** % Potency of peripheral and central analgesic properties of the tested compounds and standard references.

**Table 3**
Central analgesic properties at 10 mg kg$^{1}$ (mice body weight) indomethacin mol equivalent.

| Entry | Compd. | Latency period ± SE "standard error", second (% Protection) | | | | % Potency[a] |
|---|---|---|---|---|---|---|
| | | After 30 min. | After 60 min. | After 90 min. | After 120 min. | |
| 1 | Control | 6.68 ± 1.0 (0.0) | 7.27 ± 1.4 (0.0) | 8.91 ± 0.9 (0.0) | 9.01 ± 1.1 (0.0) | — |
| 2 | Indomethacin | 12.50 ± 2.0** (87.1) | 13.15 ± 1.6** (80.9) | 14.07 ± 1.2** (57.9) | 14.10 ± 1.9** (56.5) | 100 |
| 3 | IBU | 10.80 ± 0.8** (61.7) | 11.00 ± 1.3** (51.3) | 11.90 ± 1.5** (33.6) | 13.90 ± 2.2** (54.3) | 96.1 |
| 4 | **8ax** | 11.57 ± 1.7** (73.2) | 12.80 ± 1.6** (76.1) | 11.48 ± 1.6** (28.8) | 11.56 ± 1.4** (28.3) | 50.1 |
| 5 | **8ay** | 10.60 ± 0.7** (58.7) | 11.47 ± 1.3** (57.8) | 13.51 ± 1.5** (51.6) | 13.81 ± 1.3** (53.3) | 94.3 |
| 6 | **8az** | 13.29 ± 2.2** (99.0) | 10.52 ± 1.9* (44.7) | 10.84 ± 1.8* (21.7) | 10.65 ± 2.0* (18.2) | 32.2 |
| 7 | **8bx** | 11.67 ± 1.6** (74.7) | 11.22 ± 1.1** (54.3) | 11.79 ± 1.5** (32.3) | 11.84 ± 1.8** (31.4) | 55.6 |
| 8 | **8by** | 13.17 ± 0.9** (97.2) | 12.35 ± 2.1** (69.9) | 11.59 ± 1.7** (30.1) | 11.89 ± 1.9** (32.0) | 56.6 |
| 9 | **8bz** | 12.31 ± 1.6** (84.3) | 12.68 ± 1.8** (74.4) | 11.78 ± 2.2** (32.2) | 10.76 ± 2.5** (19.4) | 34.3 |
| 10 | **8cx** | 12.63 ± 2.4** (89.1) | 10.55 ± 2.1** (45.1) | 9.30 ± 2.0* (4.4) | 9.69 ± 1.9* (7.5) | 13.3 |
| 11 | **8cy** | 10.28 ± 1.7** (53.9) | 10.40 ± 1.3* (43.1) | 13.10 ± 1.1** (47.0) | 10.44 ± 0.9* (15.9) | 28.1 |
| 12 | **8cz** | 8.84 ± 1.5* (32.3) | 9.86 ± 1.3* (35.6) | 10.05 ± 0.7* (12.8) | 9.68 ± 1.4* (7.4) | 13.1 |
| 13 | **8dx** | 12.90 ± 1.9** (93.1) | 10.97 ± 2.6** (50.9) | 13.18 ± 2.3** (47.9) | 13.26 ± 2.6** (47.2) | 83.5 |
| 14 | **8dy** | 10.73 ± 1.4* (60.6) | 11.43 ± 2.2* (57.2) | 14.35 ± 2.8** (61.1) | 13.43 ± 2.1** (49.1) | 86.9 |
| 15 | **8dz** | 9.92 ± 2.2** (48.5) | 11.0 ± 2.6** (51.3) | 12.64 ± 1.5** (41.9) | 11.91 ± 1.3** (32.2) | 57.0 |
| 16 | **9az** | 11.48 ± 1.8** (71.9) | 12.51 ± 2.5** (72.1) | 13.05 ± 2.3** (46.5) | 13.72 ± 2.1** (52.3) | 92.6 |
| 17 | **9dz** | 11.30 ± 2.3** (69.2) | 9.27 ± 2.7* (27.5) | 10.55 ± 2.0* (18.4) | 11.12 ± 2.7* (23.4) | 41.4 |

[a] Potency is that at 120 min. relative to indomethacin. Statistical analysis was carried out by one-way ANOVA *$p$ < 0.05, **$p$ < 0.001.

### 2.6. Toxicological bio-assay

Toxicological bio-assay for the most promising anti-inflammatory agents (**8ax, 8bx**, and **8cx**) was conducted by the standard technique in mice [25,34]. Five times the anti-inflammatory dose was orally administrated (i.e. 50 mg kg$^{1}$ "mice bodyweight" indomethacin mol equivalent). None of the tested compounds reveal any mortality or toxic symptoms.

### 2.7. COX-1 and COX-2 inhibitory properties

COX-1/2 inhibitory properties were determined for the promising anti-inflammatory active agents synthesized, **8ax, 8bx**, and **8cx** (Table 5). All the tested agents show considerable inhibitory activity comparable to their precursor (ibuprofen). The results support the anti-inflammatory properties determined (Table 1). It has also been observed that enhanced selectivity was exhibited by compound **8bx** towards COX-2 compared to COX-1 (SI "selectivity index of COX-1 relative to COX-2" = 1.631). Also, enhanced SI was shown by compounds **8ax** and **8cx** (SI = 0.413, 0.213, for **8ax** and **8cx**, respectively), relative to the parent compound (SI = 0.106 for ibuprofen). From all the above observations, it can be reasonably concluded that analogs **8ax, 8bx**, and **8cx** are good anti-inflammatory candidates with potential for development into applicable agents.

### 2.8. Reduction of NO production of LPS-stimulated RAW264.7 macrophages

To assess the anti-inflammatory responses of ibuprofen conjugates on LPS-stimulated RAW264.7 macrophages, the production of NO was determined by measuring the accumulated nitrite in culture medium using Greiss reaction. LPS-stimulated control was found to induce significant nitrite production in RAW264.7 macrophages in comparison to vehicle-treated control ($P$***<0.001). In comparision, the postive control indomethacin reduced the nitrite production at 40 μg/mL ($P$*<0.05, in comparison to LPS-stimulated control). As for the ibuprofen conjugates, nitrite production was reduced at the same concentration used (40 μg/mL) for **8ax, 8bx**, and **8cx** ($P$**<0.01, $P$***<0.001, $P$***<0.001 respectively, in comparison to LPS-stimulated control) (Fig. 7A). The results also showed that the ibuprofen-quinoline conjugates reduced nitrite production compared to indomethacin. Results obtained from the

**Table 5**
COX-1 and COX-2 inhibitory properties of the tested compounds.

| Entry | Compd. | $IC_{50}$, μM ± SD | | SI[a] |
|---|---|---|---|---|
| | | COX-1 | COX-2 | |
| 1 | Indomethacin | 0.354 ± 0.01** | 3.239 ± 0.35** | 0.109 |
| 2 | IBU | 13.16 ± 0.37** | 124.2 ± 0.17** | 0.106 |
| 3 | **8ax** | 2.414 ± 0.07** | 5.842 ± 0.17** | 0.413 |
| 4 | **8bx** | 19.82 ± 0.56** | 12.15 ± 0.35** | 1.631 |
| 5 | **8cx** | 3.721 ± 0.11* | 17.44 ± 0.5* | 0.213 |

Statistical analysis was carried out by one-way ANOVA *$p$ < 0.05, **$p$ < 0.001.

[a] $SI = \frac{IC_{50(COX\ 1)}}{IC_{50(COX\ 2)}}$

**Table 4**
Ulcerogenic liability for the tested compounds.

| Entry | Compd. | Number of animals with ulcer | % Incidence of ulcer divided by 10 | Average of ulcer number | Average severity of ulcer | Ulcer index |
|---|---|---|---|---|---|---|
| 1 | Control | 0/6 | 0 | 0 | 0 | 0 |
| 2 | Indomethacin | 6/6 | 10 | 2 | 1.67 | 13.67 |
| 3 | IBU | 2/6 | 3.33 | 0.33 | 0.67 | 4.33 |
| 4 | **8ax** | 1/6 | 1.67 | 0.17 | 0.17 | 2.01 |
| 5 | **8bx** | 0 | 0 | 0 | 0 | 0 |
| 6 | **8cx** | 0 | 0 | 0 | 0 | 0 |

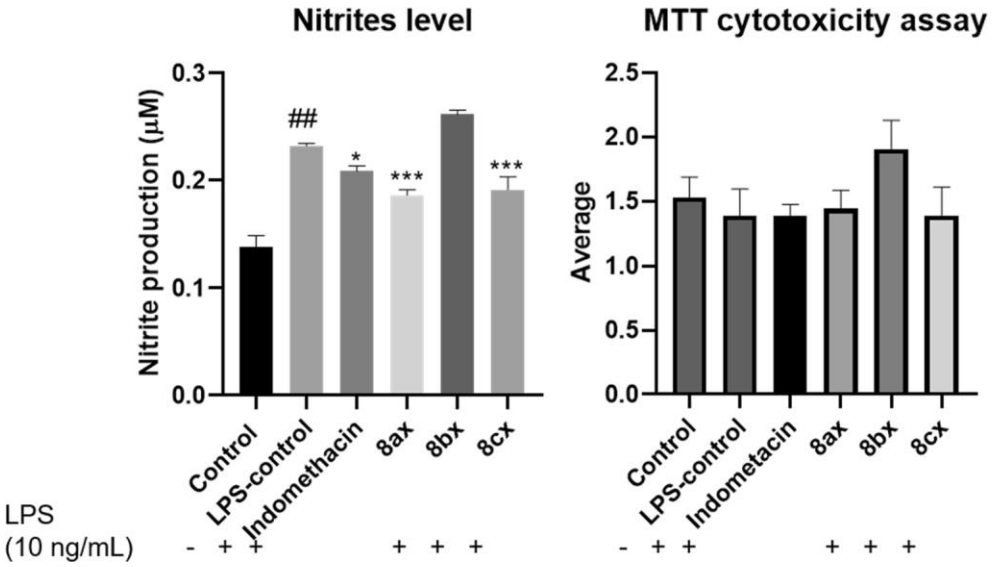


**Fig. 7.** Effects of NO production of Ibuprofen conjugates and MTT cytotoxicity on RAW264.7 macrophages. (A) After pre-treating LPS-stimulated RAW264.7 macrophages with 40 μg/mL ibuprofen conjugates and positive control, indomethacin for 24 h, nitrite content in cell supernatants was determined using the Greiss method. Values are mean ± SD (n = 3). LPS-stimulated control ***$P$ < 0.001 in comparison to vehicle-treated control; for conjugates **8ax** and **8cx**, ***$P$ < 0.001, ***$P$ < 0.001, respectively, and **8bx** showed no significant difference in comparison to LPS-stimulated cells. Significant differences in the figure are all in comparison to LPS stimulated control (indicated as ##). (B) After pre-treating LPS-stimulated RAW264.7 macrophages with 40 μg/mL ibuprofen conjugates and positive control, indomethacin for 24 h, cellular viability was determined using MTT assay. Values are mean ± SD (n = 3). All Ibuprofen conjugates and positive control indomethacin showed no significant cytotoxicity in comparison to control.

nitrite standard curve show that the nitrite concentration in the cell supernatant of vehicle-treated control cells was 12.8 μM. Additionally, in LPS-stimulated cells, nitrite level was increased significantly to 22 μM ($P$***<0.001). As for the positive control, indomethacin, and ibuprofen conjugate compounds **8ax** and **8cx**, nitrite levels were reduced to 19.6 μM, 17.5 μM and 18 μM, respectively, ($P$*<0.05, $P$***<0.001, $P$***<0.001). In contrast, ibuprofen conjugate **8bx** did not reduce nitrite production significantly in comparison to LPS-stimulated cells (24 μM). The relationship/cross-talk between COX-2 and iNOS has been previously reported [35]. In this relationship, it was also previously demonstrated that selective COX-2 inhibitors, unlike non-selective inhibitors, depress COX-2 mediated production of prostacyclin (PGI2). Consequently, and upon its production PGI2 has also been shown to induce iNOS with the subsequent production of NO [36]. Therefore, it is plausible that ibuprofen conjugate compounds **8ax** and **8cx** might have reduced NO production in part through their selective inhibition of COX-2.

To determine whether this decrease in NO production in response to the ibuprofen conjugates is due to the decrease in the cellular viability of the cells, the cytotoxicity of ibuprofen conjugates **8ax, 8bx**, and **8cx** (40 μg/mL) was measured by MTT assay on RAW264.7 macrophages. The results indicate that the positive control and ibuprofen conjugates show no cytotoxicity on RAW264.7 macrophages at the tested concentrations. Therefore, the observed decrease in NO production in the LPS-stimulated RAW264.7 cells treated with the ibuprofen conjugates **8ax, 8bx**, and **8cx** was not due to the decrease in cellular viability (Fig. 7B). Therefore, further experiments were conducted to evaluate the anti-inflammatory effect of these conjugates utilizing the same concentration of NO production.

### *2.9. Reduction of mRNA levels of inflammatory cytokines in LPS-stimulated RAW264.7 macrophages*

To evaluate the effect of ibuprofen conjugates on the pro-

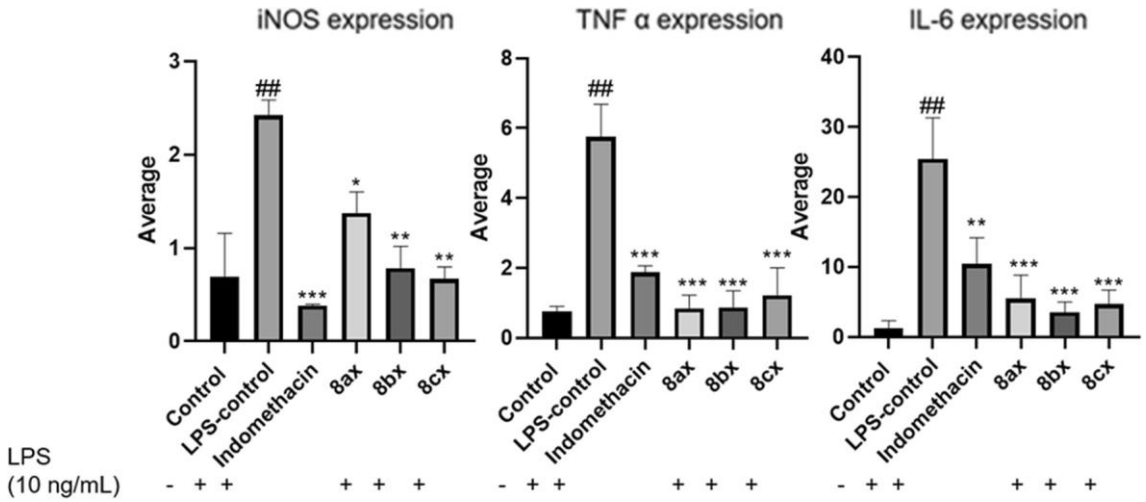


**Fig. 8.** Ibuprofen conjugates reduced iNOS (A), TNF-α (B), and IL-6 (C) mRNA expression levels in LPS-stimulated RAW264.7 macrophages. After pre-treatment of LPS-stimulated RAW264.7 macrophages (10 *n*g/mL) with 40 μg/mL of indomethacin, **8ax, 8bx**, and **8cx** for 24 h, mRNA levels of iNOS, TNF-α, and IL-6 mRNA levels were evaluated using real-time qPCR. The comparative ($2^{\Delta\Delta CT}$) method was used for evaluating the mRNA expression levels of iNOS, TNF-α, and IL-6 mRNAs (P***<0.001, P***<0.001 and P***<0.001 respectively). Significant differences in the figure are all in comparison to LPS stimulated control (indicated as ##). Values are means ± S.D. (n = 3).

inflammatory cytokines, TNF-α and IL-6 in LPS-stimulated RAW264.7 macrophages, mRNA levels of TNF-α and IL-6 were examined by real-time qPCR. For the LPS-stimulated control, there was a significant increase in the mRNA levels of TNF-α and IL-6 ($P$***<0.001). Conversely, treatment with the ibuprofen conjugates, **8ax, 8bx**, and **8cx** reduced the LPS-stimulated TNF-α and IL-6 mRNA levels in RAW264.7 macrophages (Fig. 8). For TNF-α gene expression, a significant reduction in its levels was observed in LPS-stimulated RAW264.7 cells treated with ibuprofen conjugate **8ax, 8bx**, and **8cx** ($P$***<0.001). As for IL-6 gene expression, a significant reduction in its mRNA expression levels was also observed in LPS-stimulated RAW264.7 cells treated with the ibuprofen conjugates **8ax, 8bx**, and **8cx** ($P$***<0.001). Ibuprofen conjugates also significantly reduced iNOS mRNA expression levels in LPS-stimulated RAW264.7 macrophages. iNOS is the gene encoding for the protein responsible for NO production in LPS-stimulated RAW264.7 macrophages [27]. Real-time qPCR was done to observe whether the reduction in NO production was due to a decrease in iNOS mRNA expression levels. Again, LPS-stimulated RAW264.7 macrophages showed elevated iNOS mRNA expression levels ($P$**<0.01). In contrast, pre-treatment with indomethacin, or the ibuprofen conjugates **8ax, 8bx**, and **8cx** in the presence of LPS significantly decreased the iNOS mRNA expression levels level ($P$***<0.001, $P$**<0.01, $P$*<0.05 and $P$**<0.01 respectively) in comparison to LPS-stimulated control (Fig. 8). Table 6 shows the sequences of the mRNA primers used for real-time qPCR. Forward (F) and reverse (R) sequences are shown from 5′ to 3′ for GAPDH (endogenous control), IL-6, iNOS, and TNF-α. The Primer Melting Temperature (Tm), is the temperature at which one-half of the double-stranded DNA dissociates into single-stranded DNA. Tm indicates duplex stability and a temperature above 65 °C can cause unfavorable reactions like secondary annealing. The primers used in this study have Tm in the range of 55-63 °C [37]. The qualitative comparison of the mRNA expression levels in comparison to vehicle-treated control was evaluated using the comparative $2^{\Delta\Delta CT}$ method.

### 2.10. 2D-QSAR studies

Mathematical equation(s) can be used to represent the biological properties in terms of descriptors (physicochemical parameters). This is useful for identifying the most important parameters necessary for bio-properties. This is why QSAR techniques are utilized widely in medicinal chemical studies. QSAR is capable of rationalization of the biological properties exhibited; prediction of effective agents based on the pre-assigned robust model, as well as determination of the parameters necessary for biological optimization [38,39].

### 2.11. Anti-inflammatory QSAR model

A three descriptor QSAR model was established for the anti-inflammatory properties observed for the tested conjugates **8** (Supplementary Tables S1-S3, Fig. S1). *PPSA2* (total charge weighted partial charge surface area) is a charge-related descriptor with the lowest coefficient value of all the QSAR model descriptors (coefficient = 0.0003) and can be calculated by equ. (1) [40].

**Table 6**
mRNA sequences used for RT-PCR.

| Sequence 5′ …..3′ | Primer | Tm |
|---|---|---|
| CTTTGTCAAGCTCATTTCCTGG | GAPDH F | 57 |
| TCTTGCTCAGTGTCCTTGC | GAPDH R | 58 |
| GATGCTACCAAACTGGATATAATCAG | IL6 F | 55 |
| CTCTGAAGGACTCTGGCTTTG | IL6 R | 58 |
| GGAACCTACCAGCTCACTCTGG | iNOS F | 63 |
| TGCTGAAACATTTCCTGTGCTGT | iNOS R | 60 |
| GAACTCCAGGCGGTGCCTAT | TNF-α F | 63 |
| TGAGAGGGAGGCCATTTGGG | TNF-α R | 63 |

$$PPSA2 = \sum_{A} q_A \cdot \sum_{A} S_A \; A \in \{\delta_A > 0\} \quad (1)$$

where, $S_A$ is the positively charged solvent-accessible atomic surface area, $q_A$ is the atomic partial charge.

HA dependent *HDSA*1 (hydrogen bonding donor ability) is also a charge related descriptor negatively participated in the QSAR model. The appearance of this descriptor in the QSAR model explains the enhanced anti-inflammatory properties for the tested conjugates containing fluorine and chlorine substituents among the others. This is also in line with the observed SAR mentioned. *HDSA*1 of the molecule can be calculated by equation (2) [40].

$$HDSA1 = \sum_{D} S_D \; D \in H_{Hdonor} \quad (2)$$

where, $S_D$ is the solvent accessible surface area of hydrogen bonding donor hydrogen atoms.

*HACA*1 (hydrogen bonding acceptor ability) of the molecule is also a charge-related descriptor. It can be calculated by equ. (3) [39].

$$HACA1 = \sum_{A} S_A \; A \in X_{Hacceptor} \quad (3)$$

where, $S_A$ is the solvent accessible surface area of hydrogen bonding acceptor atoms (selected by the threshold charge).

Leave one and many-out coefficient cross validation are comparable to the QSAR model coefficient value (0.978, 0.950, 0.963 for $R^2$, $R^2$cvOO and $R^2$cvMO, respectively). This supports the robustness of the QSAR model discussed. Fisher criteria ($F$) and standard deviation($s$) also validate the model.

### 2.12. Peripheral analgesic QSAR model

A robust three descriptor QSAR model ($R^2$ = 0.848, $R^2$cvOO = 0.737, $R^2$cvMO = 0.757) reports the peripheral analgesic properties of the tested conjugates (Supplementary Tables S4-S6, Fig. S2). XY Shadow / XY rectangle is a geometrical descriptor with a negative coefficient value participating in the QSAR model (coefficient = -0.953377). Thus, the higher the descriptor value, the lower the estimated bio-properties as shown in compounds **8cz** and **8dy** (descriptor values = 0.55996, 0.65827 corresponding to estimated properties = 101.85, 71.97, for **8cz** and **8dy** respectively). The Shadow area of a molecule can be determined by equ. (4) [40].

$$S_k = \frac{1}{2} \oint_{(C)} (vdp \quad \rho dv) \quad (4)$$

where, C stands for the contour of the projection of the molecule on the plane defined by two principal axes of the molecule ($k$ = *XY, XZ* or *YZ*), *v-x* or *y*, *ρ-y* or *z*.

*FNSA*2 Fractional PNSA (*PNSA*2/*TMSA*) (MOPAC PC) is a charge-related descriptor with a negative coefficient value in the QSAR model. This explains the high estimated properties of **8cz** over **8dy** (descriptor values = 1.68799, 1.28419 for **8cz** and **8dy**, respectively). This descriptor supports the SAR mentioned due to the high bio-properties of compounds that possess halogenated quinolone-conjugates over those with unsubstituted or methyl-substituted quinolone-conjugates. Fractional total charge weighted partial negative surface area can be calculated by equ. (5) [40].

$$FNSA2 = \frac{PNSA2}{TMSA} \quad (5)$$

where, *PNSA*2 stands for total charge weighted partial negatively charged molecular surface area. *TMSA* stands for total surface area.

The square root of surface area (MOPAC PC) for atom C is also a charge-related descriptor with a negative coefficient value in the QSAR model (coefficient = -0.0146294). This explains the high analgesic

properties of compound **8cz** over **8ay** (descriptor values = 50.55549, 55.97213 corresponding to estimated properties = 101.85, 70.95, for **8cz** and **8ay**, respectively). This descriptor supports the mentioned SAR due to the alkyl chain linking the quinolinyl and ibuprofen moieties. The surface-weighted charged partial positive and negative charged surface area *WPSA*1 and *WNSA*1 can be calculated by equs. (6), (7) [40].

$$WPSA1 = \frac{PPSA1.TMSA}{1000} \quad (6)$$

$$WNSA1 = \frac{PNSA1.TMSA}{1000} \quad (7)$$

here, *PPSA*1 and *PNSA*1 stand for the partial positively and negatively charged molecular surface areas, respectively. *TMSA* stands for the total molecular surface area.

Supplementary Table S5 reveals that the estimated peripheral analgesic properties are comparable to their experimentally observed results supporting the suitability of the attained QSAR model.

### 2.13. Central analgesic QSAR model

Three descriptor QSAR model was attained due to the exported agents of variable central analgesic properties (% protection = 7.4-53.3) (Supplementary Tables S7-S9, Fig. S3). Image of the Onsager-Kirkwood solvation energy is a semi-empirical descriptor with a positive coefficient value (8.305). This explains the high bio-properties of **8ay** over **8bx** (descriptor value = 0.07613, 0.01473 corresponding to estimated property = 58.4, 34.7 for compounds **8ay**, **8bx**, respectively).

Rotational entropy (300 K) is a thermodynamical descriptor with a negative sign in the attained QSAR model. This is why the compound with a high mathematical descriptor value optimizes low bio-active agent and vice versa as shown in compounds **8bx** over **8az** (descriptor value = 37.432, 39.08 corresponding to estimated property = 34.7, 23.5 for compounds **8bx**, **8az** respectively). The rotational entropy of the molecule can be calculated by equ. (8) [40].

$$S_{rot} = Nk\ln\left[\frac{\pi^{1/2}}{\sigma}\prod_{j=1}^{3}\frac{(8\pi^2 I_j kT)^{1/2}}{h^2}\right] \quad (8)$$

where, $I_j$ stands for the molecular principal moments of inertia. $\sigma$ is the molecular symmetry number. $h$ and $k$ are Planck's and Boltzmann's constants. $T$ is the absolute temperature (K).

Vibrational enthalpy (300 K)/natoms is a thermodynamical descriptor that negatively participated in the QSAR model. Although this descriptor has the lowest coefficient value (-0.040), its high varied value affects greatly the predicted properties as revealed by compounds **9az** and **8cx** (descriptor value = 290.5182, 308.0706 corresponding to estimated property = 51.5, 7.8 for compounds **9az** and **8cx**, respectively). The vibrational enthalpy of the molecule can be calculated by equ. (9) [40].

$$H_{vib} = \frac{1}{2}\sum_{j=1}^{a} h\nu_j + \frac{h\nu_j}{1 - exp(h\nu_j/2kT)} \quad (9)$$

where, $\nu_j$ is the molecular frequencies of normal vibrations. $h$ and $k$ are Planck's and Boltzmann's constants. $T$ is the absolute temperature (K).

The accuracy of the attained QSAR model is supported by the predicted biological properties compared with the experimental values (Supplementary Table S8).

### 2.14. Conclusion

In summary, a new series of ibuprofen-quinoline conjugates (**8** and **9**) were designed, synthesized, and evaluated for their anti-inflammatory and analgesic properties. Compounds **8ax, 8bx,** and **8cx** exhibited potent anti-inflammatory properties comparable to their precursor, ibuprofen. Moreover, conjugates **8bx** and **8cx** didn't show ulcerogenic liability. The most promising anti-inflammatory agents were evaluated *in vitro* as COX-1/COX-2 inhibitors and the results revealed considerable selectivity towards COX-2 compared to ibuprofen. Also, these compounds were evaluated for their suppression effect of LPS-stimulated production of NO, ROS, and the pro-inflammatory cytokines IL-6, TNF-α, and inducible nitric oxide synthase (iNOS) in RAW264.7 macrophages. The 2D-QSAR studies rationalized and supported the biological properties observed.

## 3. Experimental section

### 3.1. Chemistry

Melting points were determined on a capillary point apparatus equipped with a digital thermometer and are uncorrected. NMR spectra were recorded in $CDCl_3$ on a Bruker spectrometer operating at 500 MHz for $^1H$ (with TMS as an internal standard) and 125 MHz for $^{13}C$. The microwave-assisted reaction was carried out with a single-mode cavity Discover Microwave Synthesizer (CEM Corporation, NC). The reaction mixtures were transferred into a 10 mL glass pressure microwave tube equipped with a magnetic stir bar. The tube was closed with a silicon septum and the reaction mixture was subjected to microwave irradiation (Discover mode; run time: 120 s; Power Max-cooling mode). High-resolution mass spectra were recorded with a TOF analyzer spectrometer by using electron spray mode. Single-crystal X-ray diffraction data were collected using an Agilent SuperNova Dual Atlas diffractometer with mirror monochromated Cu radiation.

Derivatives of 2-(trifluoromethyl)quinolin-4(1*H*)-one **3a-d** were prepared according to the reported procedure [29,30].

#### 3.1.1. General procedure for alkylation of 2-(trifluoromethyl)quinolin-4 (1H)-ones *3a-d*

A mixture of 2-trifluoromethyl-4-quinolinone **3a-d** (0.90 mmol), dibromoalkane (0.90 mmol), and anhydrous $K_2CO_3$ (1.80 mmol) was stirred in DMF (5 mL) in a round-bottomed flask for 6-8 h at room temperature. The reaction mixture was poured on ice-cold water and the contents were then extracted with diethyl ether, washed with brine solution, and dried over anhydrous sodium sulfate. The solvent was removed under reduced pressure and the crude residue was purified by column chromatography. The column was packed in hexanes and eluted with hexanes: ethyl acetate mixture. All products were isolated and identified as compounds **4, 5,** and **6**.

#### 3.1.2. 4-(3-Bromopropoxy)-2-(trifluoromethyl)quinoline *(4ax)*

White microcrystals (76 % yield), m.p. 87 °C. IR ($\nu_{max}$/cm$^1$): 3100, 2950, 2876, 1591, 1509, 1479, 1365. $^1H$ NMR (500 MHz, $CDCl_3$) δ: 8.25 (d, *J* = 8.8 Hz, 1H), 8.18 (d, *J* = 8.5 Hz, 1H), 7.85-7.78 (m, 1H), 7.64 (t, *J* = 7.9 Hz, 1H), 7.10 (s, 1H), 4.46 (t, *J* = 5.8 Hz, 2H), 3.72 (t, *J* = 6.3 Hz, 2H), 2.58-2.52 (m, 2H). $^{13}C$ NMR (125 MHz, $CDCl_3$) δ: 162.76, 149.08 (q, *J* = 34.3 Hz), 148.17, 131.02, 129.74, 127.61, 121.70, 121.61, 121.52 (q, *J* = 275.3 Hz), 96.78, 66.47, 31.81, 29.15. HRMS: *m*/*z* for $C_{13}H_{11}BrF_3NO$ $[M + H]^+$ Calcd.: 333.9976. Found: 333.9972.

#### 3.1.3. 4-(4-Bromobutoxy)-2-(trifluoromethyl)quinoline *(4ay)*

White microcrystals (72 % yield), m.p. 99 °C. IR ($\nu_{max}$/cm$^1$): 3050, 2939, 2897, 1591, 1575, 1512, 1372. $^1H$ NMR (500 MHz, $CDCl_3$) δ: 8.26 (d, *J* = 8.4 Hz, 1H), 8.17 (d, *J* = 8.5 Hz, 1H), 7.84-7.79 (m,1H), 7.64 (t, *J* = 7.6 Hz, 1H), 7.05 (s, 1H), 4.33 (t, *J* = 5.4 Hz, 2H), 3.57 (t, *J* = 6.0 Hz, 2H), 2.21-2.17 (m, 4H). $^{13}C$ NMR (125 MHz, $CDCl_3$) δ: 162.98, 149.07 (q, *J* = 34.1 Hz), 148.15, 130.97, 129.68, 127.56, 121.81, 121.68, 121.55 (q, *J* = 275.5 Hz), 96.65, 68.12, 32.99, 29.37, 27.46. HRMS: *m*/*z* for $C_{14}H_{13}BrF_3NO$ $[M + H]^+$ Calcd.: 348.0133. Found: 348.0137.

#### 3.1.4. 4-(6-Bromohexoxy)-2-(trifluoromethyl)quinoline *(4az)*

White microcrystals (77 % yield), m.p. 79 °C. IR ($\nu_{max}$/cm$^1$): 3089,

$$\prod$$

$$\sum$$

2937, 2898, 1598, 1577, 1478, 1412. $^1$H NMR (500 MHz, $CDCl_3$) δ: 8.28 (d, *J* = 8.3 Hz, 1H), 8.17 (d, *J* = 8.5 Hz, 1H), 7.84-7.78 (m, 1H), 7.64 (t, *J* = 7.6 Hz, 1H), 7.06 (s, 1H), 4.30 (t, *J* = 6.3 Hz, 2H), 3.47 (t, *J* = 6.7 Hz, 2H), 2.05-2.00 (m, 2H), 1.99-1.94 (m, 2H), 1.66-1.62 (m, 4H). $^{13}$C NMR (125 MHz, $CDCl_3$) δ: 163.19, 149.10 (q, *J* = 34.3 Hz), 148.15, 130.90, 129.66, 127.44, 121.69, 121.79, 121.58 (q, *J* = 275.5 Hz), 96.65, 68.90, 33.62, 32.60, 28.68, 27.88, 25.36. HRMS: *m*/*z* for $C_{16}H_{17}BrF_3NO$ $[M + H]^+$ Calcd.: 376.0446. Found: 376.0449.

*3.1.5. 4-(3-Bromopropoxy)-6-fluoro-2-trifluoromethyl)quinoline* ***(4bx)***

White microcrystals (79 % yield), m.p. 91 °C. IR ($\nu_{max}$/cm$^1$): 3100, 2932, 2888, 1598, 1578, 1517, 1409. $^1$H NMR (500 MHz, $CDCl_3$) δ: 8.19-8.15 (m, 1H), 7.82-7.80 (m, 1H), 7.58-7.56 (m, 1H), 7.11 (s, 1H), 4.48-4.45 (m, 2H), 3.71 (t, *J* = 6.3 Hz, 2H), 2.57-2.52 (m, 2H). $^{13}$C NMR (125 MHz, $CDCl_3$) δ: 162.29, 161.28 (d, *J* = 254.0 Hz), 148.52 (q, *J* = 34.4 Hz), 145.17, 132.43 (d, *J* = 9.2 Hz), 122.55 (d, *J* = 9.8 Hz), 121.44 (q, *J* = 275.5 Hz), 121.23 (d, *J* = 25.7 Hz), 105.71 (d, *J* = 23.8 Hz), 97.22, 66.65, 31.70, 29.05. HRMS: *m*/*z* for $C_{13}H_{10}BrF_4NO$ $[M + H]^+$ Calcd.: 351.9882, Found: 351.9887.

*3.1.6. 4-(4-Bromobutoxy)-6-fluoro-2-(trifluoromethyl)quinoline* ***(4by)***

White microcrystals (76 % yield), m.p. 75 °C. IR ($\nu_{max}$/cm$^1$): 3090, 2929, 2895, 1599, 1577, 1478, 1412. $^1$H NMR (500 MHz, $CDCl_3$) δ: 8.16 - 8.14 (m, 1H), 7.83-7.81 (m, 1H), 7.55 (t, *J* = 8.6 Hz, 1H), 7.05 (s, 1H), 4.43-4.21 (m, 2H), 3.56 -3.54 (m, 2H), 2.19 -2.16 (m, 4H). $^{13}$C NMR (125 MHz, $CDCl_3$) δ: 162.51, 161.25 (d, *J* = 250.1 Hz), 148.52 (q, *J* = 34.4 Hz), 145.18, 132.40 (d, *J* = 9.2 Hz), 122.64 (d, *J* = 10.1 Hz), 121.46 (q, *J* = 275.2 Hz), 121.20 (d, *J* = 25.8 Hz), 105.82 (d, *J* = 23.8 Hz) 0.97.10, 68.29, 32.88, 29.27, 27.41. HRMS: *m*/*z* for $C_{14}H_{12}BrF_4NO$ $[M + H]^+$ Calcd.: 366.0038, Found: 366.0042.

*3.1.7. 4-(6-Bromohexoxy)-6-fluoro-2-(trifluoromethyl)quinoline* ***(4bz)***

White crystals (81 % yield), m.p. 69 °C. IR ($\nu_{max}$/cm$^1$): 3089, 2937, 2898, 1598, 1577, 1478, 1412. $^1$H NMR (500 MHz, $CDCl_3$) δ: 8.17 (dd, *J* = 9.2, 5.2 Hz, 1H), 7.85 (dd, *J* = 9.2, 2.8 Hz, 1H), 7.60-7.54 (m, 1H), 7.06 (s, 1H), 4.30 (t, *J* = 6.3 Hz, 2H), 3.48 (t, *J* = 6.7 Hz, 2H), 2.06-2.00 (m, 2H), 1.99-1.94 (m, 2H), 1.75-1.52 (m, 4H). $^{13}$C NMR (125 MHz, $CDCl_3$) δ: 162.71, 161.20 (d, *J* = 249.9 Hz), 148.53 (q, *J* = 34.4 Hz), 145.16, 132.33 (d, *J* = 9.1 Hz), 122.74 (d, *J* = 9.8 Hz), 121.50 (q, *J* = 275.3 Hz), 121.12 (d, *J* = 25.8 Hz), 105.88 (d, *J* = 23.7 Hz), 97.07, 69.08, 33.59, 32.52, 28.65, 27.87, 25.32. HRMS: *m*/*z* for $C_{16}H_{16}BrF_4NO$ $[M + H]^+$ Calcd.: 394.0351. Found: 394.0347.

*3.1.8. 4-(3-Bromopropoxy)-6-chloro-2-(trifluoromethyl)quinoline* ***(4cx)***

White microcrystals (85 % yield), m.p. 105 °C. IR ($\nu_{max}$/cm$^1$): 3030, 2925, 2879, 1592, 1501, 1459, 1375. $^1$H NMR (500 MHz, $CDCl_3$) δ: 8.20 (d, *J* = 2.4 Hz, 1H), 8.11 (d, *J* = 9.0 Hz, 1H), 7.75 (dd, *J* = 9.0, 2.4 Hz, 1H), 7.12 (s, 1H), 4.47 (t, *J* = 5.8 Hz, 2H), 3.72 (t, *J* = 6.3 Hz, 2H), 2.58-2.53 (m, 2H). $^{13}$C NMR (125 MHz, $CDCl_3$) δ: 161.96, 149.34 (q, *J* = 34.3 Hz), 146.56, 133.81, 132.01, 131.39, 122.31, 121.39 (q, *J* = 275.6 Hz), 120.90, 97.52, 66.75, 31.69, 29.08. HRMS: *m*/*z* for $C_{13}H_{10}BrClF_3NO$ $[M + H]^+$ Calcd.: 367.9586. Found: 367.9588.

*3.1.9. 4-(4-Bromobutoxy)-6-chloro-2-(trifluoromethyl)quinoline* ***(4cy)***

White microcrystals (78 % yield), m.p. 91 °C. IR ($\nu_{max}$/cm$^1$): 3078, 2924, 2877, 1591, 1572, 1501, 1411. $^1$H NMR (500 MHz, $CDCl_3$) δ: 8.21 (d, *J* = 2.4 Hz, 1H), 8.09 (d, *J* = 9.0 Hz, 1H), 7.74 (dd, *J* = 9.0, 2.4 Hz, 1H), 7.07 (s, 1H), 4.33-4.30 (m, 2H), 3.58 (t, *J* = 5.8 Hz, 2H), 2.21-2.19 (m, 4H). $^{13}$C NMR (125 MHz, $CDCl_3$) δ: 162.16, 149.31 (q, *J* = 34.4 Hz), 146.52, 133.73, 131.95, 131.32, 122.37, 121.38 (q, *J* = 275.6 Hz), 121.01, 97.4, 68.40, 32.90, 29.23, 27.39. HRMS: *m*/*z* for $C_{14}H_{12}BrClF_3NO$ $[M + H]^+$ Calcd.: 381.9743. Found: 381.9742.

*3.1.10. 4-(6-Bromohexoxy)-6-chloro-2-(trifluoromethyl)quinoline* ***(4cz)***

White microcrystals (73 % yield), m.p. 81 °C. IR ($\nu_{max}$/cm$^1$): 3008, 2995, 2889, 1591, 1508, 1459, 1374. $^1$H NMR (500 MHz, $CDCl_3$) δ: 8.23 (d, *J* = 2.3 Hz, 1H), 8.10 (d, *J* = 9.0 Hz, 1H), 7.74 (dd, *J* = 9.0, 2.3 Hz, 1H), 7.07 (s, 1H), 4.30 (t, *J* = 6.3 Hz, 2H), 3.48 (t, *J* = 6.7 Hz, 2H), 2.08-2.00 (m, 2H), 2.01-1.93 (m, 2H), 1.69-1.61 (m, 4H). $^{13}$C NMR (125 MHz, $CDCl_3$) δ: 162.38, 139.45 (q, *J* = 34.4 Hz), 146.54, 133, 62, 131.89, 131.30, 122.49, 122.02 (q, *J* = 275.6 Hz), 121.10, 97.38, 69.20, 33.59, 32.55, 28.63, 27.87, 25.32. HRMS: *m*/*z* for $C_{16}H_{16}BrClF_3NO$ $[M + H]^+$ Calcd.: 410.0056. Found: 410.0060.

*3.1.11. 4-(3-Bromopropoxy)-6-methyl-2-(trifluoromethyl)quinoline* ***(4dx)***

White microcrystals (83 % yield), m.p. 98 °C. IR ($\nu_{max}$/cm$^1$): 3055, 2984, 2867, 1575, 1508, 1409, 1371. $^1$H NMR (500 MHz, $CDCl_3$) δ: 8.07 (d, *J* = 8.6 Hz, 1H), 7.99 (s, 1H), 7.65 (d, *J* = 8.6 Hz, 1H), 7.07 (s, 1H), 4.44 (t, *J* = 5.8 Hz, 2H), 3.73 (t, *J* = 6.3 Hz, 2H), 2.60 (s, 3H), 2.59-2.50 (m, 2H). $^{13}$C NMR (125 MHz, $CDCl_3$) δ: 162.14, 148.14 (q, *J* = 34.1 Hz), 146.72, 137.88, 133.21, 129.46, 121.59 (q, *J* = 279.8 Hz), 121.55, 120.44, 96.77, 66.37, 31.85, 29.25, 21.94. HRMS: *m*/*z* for $C_{14}H_{13}BrF_3NO$ $[M + H]^+$ Calcd.: 348.0133. Found: 348.0131.

*3.1.12. 4-(4-Bromobutoxy)-6-methyl-2-(trifluoromethyl)quinoline* ***(4dy)***

White microcrystals (70 % yield), m.p. 81 °C. IR ($\nu_{max}$/cm$^1$): 3010, 2985, 2916, 1591, 1509, 1479, 1411. $^1$H NMR (500 MHz, $CDCl_3$) δ: 8.06 (d, *J* = 8.6 Hz, 1H), 8.01 (s, 1H), 7.64 (dd, *J* = 8.6, 1.9 Hz, 1H), 7.03 (s, 1H), 4.32 (t, *J* = 5.4 Hz, 2H), 3.59 (t, *J* = 6.0 Hz, 2H), 2.60 (s, 3H), 2.27-2.15 (m, 4H). $^{13}$C NMR (125 MHz, $CDCl_3$) δ: 162.38, 148.14 (q, *J* = 34.4 Hz), 146.71, 137.83, 133.18, 129.42, 121.66 (q, *J* = 275.5 Hz), 121.60, 120.58, 96.65, 68.03, 33.04, 29.38, 27.46, 21.89. HRMS: *m*/*z* for $C_{15}H_{15}BrF_3NO$ $[M + H]^+$ Calcd.: 362.0289. Found: 362.0287.

*3.1.13. 4-(6-Bromohexoxy)-6-methyl-2-(trifluoromethyl)quinoline* ***(4dz)***

White microcrystals (80 % yield), m.p. 72 °C. IR ($\nu_{max}$/cm$^1$): 3067, 2926, 2887, 1591, 1575, 1509, 1412. $^1$H NMR (500 MHz, $CDCl_3$) δ: 8.06 (d, *J* = 8.6 Hz, 1H), 8.02 (s, 1H), 7.63 (dd, *J* = 8.6, 1.8 Hz, 1H), 7.02 (s, 1H), 4.28 (t, *J* = 6.3 Hz, 2H), 3.48 (t, *J* = 6.7 Hz, 2H), 2.60 (s, 3H), 2.08-2.00 (m, 2H), 2.01-1.93 (m, 2H), 1.65-1.63 (m, 4H). $^{13}$C NMR (125 MHz, $CDCl_3$) δ: 162.59, 148.16 (q, *J* = 34.0 Hz), 146.70, 137.69, 133.11, 129.37, 121.71, 121.69 (q, *J* = 275.5 Hz), 120.65, 96.64, 68.81, 33.63, 32.59, 28.69, 27.89, 25.37, 21.89. HRMS: *m*/*z* for $C_{17}H_{19}BrF_3NO$ $[M + H]^+$ Calcd.: 390.0602. Found: 390.0605.

*3.1.14. 1-(3-Bromopropyl)-2-(trifluoromethyl)quinolin-4(1H)-one* ***(5ax)***

Colourless oil (15 % yield). IR ($\nu_{max}$/cm$^1$): 3017, 2990, 2891, 1667, 1598, 1454, 1406. $^1$H NMR (500 MHz, $CDCl_3$) δ: 7.91 (d, *J* = 8.2 Hz, 1H), 7.74-7.67 (m, 1H), 7.59 (d, *J* = 8.6 Hz, 1H), 7.37 (t, *J* = 7.5 Hz, 1H), 7.12 (s, 1H), 4.52-4.49 (m, 2H), 3.59 (t, *J* = 6.3 Hz, 2H), 2.38-2.32 (m, 2H). $^{13}$C NMR (125 MHz, $CDCl_3$) δ: 160.49, 139.72, 137.26 (q, *J* = 31.5 Hz), 131.92, 126.16, 123.0, 122.43 (q, *J* = 275.5 Hz), 120.96, 115.51, 114.71, 41.78, 30.56, 30.06. HRMS: *m*/*z* for $C_{13}H_{11}BrF_3NO$ $[M + H]^+$ Calcd.: 333.9976. Found: 333.9979.

*3.1.15. 1-(4-Bromobutyl)-2-(trifluoromethyl)quinolin-4(1H)-one* ***(5ay)***

Colourless oil (9 % yield). IR ($\nu_{max}$/cm$^1$): 3007, 2995, 2880, 1621, 1576, 1467, 1408. $^1$H NMR (500 MHz, $CDCl_3$) δ: 8.04 (d, *J* = 8.4 Hz, 1H), 7.93 (d, *J* = 8.4 Hz, 1H), 7.75-7.67 (m, 1H), 7.53-7.48 (m, 1H), 7.26 (s, 1H), 4.57 (t, *J* = 6.2 Hz, 2H), 3.54 (t, *J* = 6.6 Hz, 2H), 2.15-2.09 (m, 2H), 2.08-2.01 (m, 2H). $^{13}$C NMR (125 MHz, $CDCl_3$) δ: 160.84, 147.55, 137.13 (q, *J* = 31.8 Hz), 130.36, 128.08, 125.30, 124.06, 123.09 (q, *J* = 274.5 Hz), 119.77, 111.61 (q, *J* = 5.6 Hz), 65.43, 33.31, 29.49, 27.54. HRMS: *m*/*z* for $C_{14}H_{13}BrF_3NO$ $[M + H]^+$ Calcd.: 348.0133. Found: 348.0130.

*3.1.16. 1-(6-Bromohexyl)-2-(trifluoromethyl)quinolin-4(1H)-one* ***(5az)***

Colourless oil (15 % yield). IR ($\nu_{max}$/cm$^1$): 3018, 2980, 2899, 1622, 1587, 1458, 1410. $^1$H NMR (500 MHz, $CDCl_3$) δ: 8.03 (d, *J* = 8.4 Hz, 1H), 7.93 (d, *J* = 8.3 Hz, 1H), 7.74-7.69 (m, 1H), 7.52-7.48 (m, 1H), 7.26 (s, 1H), 4.53 (t, *J* = 6.6 Hz, 2H), 3.46 (t, *J* = 6.8 Hz, 2H), 1.97-1.91 (m, 2H), 1.90-1.86 (m, 2H), 1.60-1.56 (m, 4H). $^{13}$C NMR (125 MHz,

$CDCl_3$) δ: 161.04, 147.64, 137.01 (q, *J* = 31.8 Hz), 130.29, 128.07, 125.18, 124.06, 123.02 (q, *J* = 297.6 Hz), 119.72, 111.72 (q, *J* = 5.6 Hz), 66.32, 33.78, 32.71, 28.68, 27.94, 25.34. HRMS: *m*/*z* for $C_{16}H_{17}BrF_3NO$ $[M + H]^+$ Calcd.: 376.0446. Found: 376.0444.

### *3.1.17. 1-(4-Bromobutyl)-6-methyl-2-(trifluoromethyl)quinolin-4(1H)-one **(5dy)***

Colourless oil (23 % yield). IR ($\nu_{max}$/$cm^1$): 3022, 2986, 2894, 1620, 1575, 1463, 1415. $^1H$ NMR (500 MHz, $CDCl_3$) δ: 7.82 (d, *J* = 8.5 Hz, 1H), 7.79 (s, 1H), 7.56 (d, *J* = 8.5 Hz, 1H), 7.23 (s, 1H), 4.55 (t, *J* = 6.2 Hz, 2H), 3.54 (t, *J* = 6.6 Hz, 2H), 2.56 (s, 3H), 2.14-2.08 (m, 2H), 2.05-2.00 (m, 2H). $^{13}C$ NMR (125 MHz, $CDCl_3$) δ: 160.39, 145.93, 136.51 (q, *J* = 31.6 Hz), 136.14, 132.37, 127.77, 123.20 (q, *J* = 274.5 Hz), 123.17, 119.74, 111.39 (q, *J* = 5.7 Hz), 65.27, 33.36, 29.52, 27.57, 21.69. HRMS: *m*/*z* for $C_{15}H_{15}BrF_3NO$ $[M + H]^+$ Calcd.: 362.0289. Found: 362.0294.

### *3.1.18. 1-(6-Bromohexyl)-6-methyl-2-(trifluoromethyl)quinolin-4(1H)-one **(5dz)***

Yellow microcrystals (11 % yield), m.p. 61 °C. IR ($\nu_{max}$/$cm^1$): 3022, 2936, 2884, 1620, 1575, 1462, 1401. $^1H$ NMR (500 MHz, $CDCl_3$) δ: 7.83 (d, *J* = 8.5 Hz, 1H), 7.79 (s, 1H), 7.55 (dd, *J* = 8.5, 1.6 Hz, 1H), 7.23 (s, 1H), 4.51 (t, *J* = 6.6 Hz, 2H), 3.46 (t, *J* = 6.8 Hz, 2H), 2.55 (s, 3H), 1.99-1.91 (m, 2H), 1.90-1.87 (m, 2H), 1.62-1.51 (m, 4H). $^{13}C$ NMR (125 MHz, $CDCl_3$) δ: 160.58, 146.00, 136.41 (q, *J* = 31.5 Hz), 135.00, 127.76, 123.20 (q, *J* = 274.7 Hz), 123.16, 119.68, 111.51 (q, *J* = 5.8 Hz), 66.18, 33.77, 32.72, 28.72, 27.95, 25.35, 21.68. HRMS: *m*/*z* for $C_{17}H_{19}BrF_3NO$ $[M + H]^+$ Calcd.: 390.0602. Found: 390.0606.

### *3.1.19. 1,4-Bis((2-(trifluoromethyl)quinolin-4-yl)oxy)butane **(6ay)***

Yellow oil (9 % yield). IR ($\nu_{max}$/$cm^1$): 3011, 2924, 2885, 1736, 1593, 1575, 1416. $^1H$ NMR (500 MHz, $CDCl_3$) δ: 8.20 (d, *J* = 8.0 Hz, 2H), 8.15 (d, *J* = 8.5 Hz, 2H), 7.83-7.77 (m, 2H), 7.62-7.55 (m, 2H), 7.07 (s, 2H), 4.48-4.44 (m, 4H), 2.37-2.32 (m, 4H). $^{13}C$ NMR (126 MHz, $CDCl_3$) δ: 162.90, 148.98 (q, 25.9 Hz), 148.10, 131.03, 129.68, 127.56, 121.59, 121.54, 121.53 (q, *J* = 276.3 Hz), 96.67, 68.52, 25.78. HRMS: *m*/*z* for $C_{24}H_{18}F_6N_2O_2$ $[M + H]^+$ Calcd.: 481.1272. Found: 481.1271.

### *3.1.20. 1,3-Bis((6-fluoro-2-(trifluoromethyl)quinolin-4-yl)oxy)propane **(6bx)***

White microcrystals (39 % yield), m.p. 204 °C. IR ($\nu_{max}$/$cm^1$): 3033, 2975, 2897, 1737, 1595, 1577, 1482. $^1H$ NMR (500 MHz, $CDCl_3$) δ: 8.18 (dd, *J* = 9.2, 5.2 Hz, 2H), 7.85 (dd, *J* = 9.2, 2.8 Hz, 2H), 7.61-7.56 (m, 2H), 7.14 (s, 2H), 4.61 (t, *J* = 5.9 Hz, 4H), 2.72 (m, 2H). $^{13}C$ NMR (126 MHz, $CDCl_3$) δ: 162.29, 161.27 (d, *J* = 231.9 Hz), 145.17, 132.49 (d, *J* = 9.2 Hz), 122.49 (d, *J* = 10.1 Hz), 121.38 (q, *J* = 274.4 Hz), 121.37 (d, *J* = 25.8 Hz), 105.75, 105.57, 97.23, 65.47, 28.62. HRMS: *m*/*z* for $C_{23}H_{14}F_8N_2O_2$ $[M + H]^+$ Calcd.: 503.0928. Found: 503.0922.

### *3.1.21. 1,6-Bis((6-methyl-2-(trifluoromethyl)quinolin-4-yl)oxy)hexane **(6dz)***

Yellow oil (22 % yield). IR ($\nu_{max}$/$cm^1$): 3023, 2923, 2874, 1737, 1575, 1905, 1413. $^1H$ NMR (500 MHz, $CDCl_3$) δ: 8.09 (d, *J* = 8.6 Hz, 2H), 7.98 (s, 2H), 7.62 (dd, *J* = 8.6, 1.9 Hz, 2H), 7.04 (s, 2H), 4.33 (t, *J* = 6.3 Hz, 4H), 2.53 (s, 6H), 2.15-2.08 (m, 4H), 1.80-1.77 (m, 4H). $^{13}C$ NMR (126 MHz, $CDCl_3$) δ: 162.78, 148.25 (q, 25.9 Hz), 146.39, 137.85, 133.30, 129.12, 121.65 (q, *J* = 275.3 Hz), 121.63, 120.54, 96.66, 68.89, 28.75, 25.87, 21.81. HRMS: *m*/*z* for $C_{28}H_{26}F_6N_2O_2$ $[M + H]^+$ Calcd.: 537.1898. Found: 537.1901.

### *3.1.22. General procedure for the synthesis of ibuprofen-quinoline hybrids **8** and **9***

A dried heavy-walled Pyrex tube containing a small stir bar was charged with the respective bromo-derivative (**4** and **5**) (1.1 mmol) and ibuprofen **7** (0.97 mmol) dissolved in DMF (3 mL) along with anhydrous potassium carbonate (2.4 mmol). The reaction mixture was exposed to microwave irradiation (20 W) at 70 °C for 2 h. The mixture was allowed to cool then quenched with ice-cold water (20 mL). The product was extracted with ethyl acetate and the organic layer was washed with brine solution and dried over anhydrous sodium sulfate. The solvent was removed under reduced pressure and the targeted compounds **8** and **9** were obtained after column chromatography purification (hexanes/ethyl acetate 9:1).

### *3.1.23. 3-((2-(Trifluoromethyl)quinolin-4-yl)oxy)propyl 2-(4-isobutylphenyl)propanoate **(8ax)***

Colourless oil (88 % yield). IR ($\nu_{max}$/$cm^1$): 3005, 2991, 2929, 2887, 1730, 1595, 1513, 1368. $^1H$ NMR (500 MHz, $CDCl_3$) δ: 8.21 (d, *J* = 8.1 Hz, 1H), 8.16 (d, *J* = 8.5 Hz, 1H), 7.80-7.77 (m, 1H), 7.61 (t, *J* = 7.6 Hz, 1H), 7.19 (d, *J* = 8.0 Hz, 2H), 7.04 (d, *J* = 8.0 Hz, 2H), 6.95 (s, 1H), 4.46-4.31 (m, 2H), 4.20-4.11 (m, 2H), 3.74 (q, *J* = 7.2 Hz, 1H), 2.40 (d, *J* = 7.2 Hz, 2H), 2.32-2.20 (m, 2H), 1.88-1.71 (m, 1H), 1.51 (d, *J* = 7.2 Hz, 3H), 0.87 (d, *J* = 6.6 Hz, 6H). $^{13}C$ NMR (125 MHz, $CDCl_3$) δ: 174.63, 162.84, 148.97 (q, *J* = 34.1 Hz), 148.12, 140.72, 137.64, 130.96, 129.62, 129.33, 127.54, 127.04, 121.83, 121.62, 121.59 (q, *J* = 275.6 Hz), 96.58, 65.19, 60.72, 45.12, 44.89, 30.13, 28.18, 22.28, 18.23. HRMS: *m*/*z* for $C_{26}H_{28}F_3NO_3$ $[M + H]^+$ Calcd.: 460.2021. Found: 460.2018.

### *3.1.24. 4-((2-(Trifluoromethyl)quinolin-4-yl)oxy)butyl 2-(4-isobutylphenyl)propanoate **(8ay)***

Colourless oil (86 % yield). IR ($\nu_{max}$/$cm^1$): 3064, 2956, 2880, 1727, 1593, 1574, 1468, 1366. $^1H$ NMR (500 MHz, $CDCl_3$) δ: 8.22 (d, *J* = 8.2 Hz, 1H), 8.16 (d, *J* = 8.5 Hz, 1H), 7.83-7.76 (m, 1H), 7.61 (t, *J* = 7.6 Hz, 1H), 7.23 (d, *J* = 8.0 Hz, 2H), 7.09 (d, *J* = 8.0 Hz, 2H), 7.00 (s, 1H), 4.29-4.16 (m, 4H), 3.73 (q, *J* = 7.2 Hz, 1H), 2.42 (d, *J* = 7.2 Hz, 2H), 1.95-1.90 (m, 4H), 1.90-1.79 (m, 1H), 1.52 (d, *J* = 7.2 Hz, 3H), 0.88 (d, *J* = 6.6 Hz, 6H). $^{13}C$ NMR (125 MHz, $CDCl_3$) δ: 174.73, 163.03, 149.03 (q, *J* = 34.1 Hz), 148.13, 140.59, 137.78, 130.91, 129.62, 129.33, 127.47, 127.12, 121.86, 121.70, 121.59 (q, *J* = 275.5 Hz), 96.59, 68.42, 63.94, 45.20, 44.97, 30.87, 30.15, 25.39, 22.30, 18.35. HRMS: *m*/*z* for $C_{27}H_{30}F_3NO_3$ $[M + H]^+$ Calcd.: 474.2178. Found: 474.2181.

### *3.1.25. 6-((2-(Trifluoromethyl)quinolin-4-yl)oxy)hexyl 2-(4-isobutylphenyl)propanoate **(8az)***

Colourless oil (79 % yield). IR ($\nu_{max}$/$cm^1$): 3020, 2951, 2880, 1731, 1593, 1512, 1470. $^1H$ NMR (500 MHz, $CDCl_3$) δ: 8.26 (d, *J* = 8.4 Hz, 1H), 8.17 (d, *J* = 8.5 Hz, 1H), 7.82-7.78 (m, 1H), 7.63 (t, *J* = 7.6 Hz, 1H), 7.23 (d, *J* = 8.0 Hz, 2H), 7.10 (d, *J* = 8.0 Hz, 2H), 7.04 (s, 1H), 4.23 (t, *J* = 6.4 Hz, 2H), 4.20-4.06 (m, 2H), 3.72 (q, *J* = 7.2 Hz, 1H), 2.45 (d, *J* = 7.2 Hz, 2H), 1.99-1.89 (m, 2H), 1.90-1.79 (m, 1H), 1.73-1.63 (m, 2H), 1.63-1.53 (m, 2H), 1.52 (d, *J* = 7.2 Hz, 3H), 1.46-1.36 (m, 2H), 0.90 (d, *J* = 6.6 Hz, 6H). $^{13}C$ NMR (125 MHz, $CDCl_3$) δ: 174.80, 163.21, 149.08 (q, *J* = 34.1 Hz), 148.15, 140.49, 137.91, 130.89, 129.63, 129.28, 127.42, 127.16, 121.93, 121.79, 121.62 (q, *J* = 275.5 Hz), 96.62, 68.93, 64.42, 45.21, 45.02, 30.18, 28.67, 28.45, 25.62, 25.52, 22.35, 18.44. HRMS: *m*/*z* for $C_{29}H_{34}F_3NO_3$ $[M + H]^+$ Calcd.: 502.2491. Found: 502.2495.

### *3.1.26. 3-((6-Fluoro-2-(trifluoromethyl)quinolin-4-yl)oxy)propyl-2-(4-isobutylphenyl)propanoate **(8bx)***

White microcrystals (89 % yield), m.p. 68 °C. IR ($\nu_{max}$/$cm^1$): 3005, 2975, 2895, 1734, 1600, 1517, 1479, 1380. $^1H$ NMR (500 MHz, $CDCl_3$) δ: 8.10 (dd, *J* = 9.2, 5.2 Hz, 1H), 7.72 (dd, *J* = 9.2, 2.8 Hz, 1H), 7.49 (td, *J* = 9.1, 2.8 Hz, 1H), 7.19 (d, *J* = 8.0 Hz, 2H), 7.04 (d, *J* = 8.0 Hz, 2H), 6.93 (s, 1H), 4.46-4.31 (m, 2H), 4.14-4.11 (m, 2H), 3.74 (q, *J* = 7.2 Hz, 1H), 2.39 (d, *J* = 7.2 Hz, 2H), 2.24 (p, *J* = 6.0 Hz, 2H), 1.83-1.74 (m, 1H), 1.51 (d, *J* = 7.2 Hz, 3H), 0.86 (d, *J* = 6.7 Hz, 6H). $^{13}C$ NMR (125 MHz, $CDCl_3$) δ: 174.52, 162.27 (d, *J* = 5.2 Hz), 161.12 (d, *J* = 250.2 Hz), 148.32 (qd, *J* = 34.3, 2.5 Hz), 145.03, 140.66, 137.69, 132.22 (d, *J* = 9.1 Hz), 129.30, 127.04, 122.46 (d, *J* = 9.9 Hz), 121.52 (q, *J* = 275.4 Hz), 121.02 (d, *J* = 25.8 Hz), 105.71 (d, *J* = 23.8 Hz), 96.93 (d, *J* = 1.7

Hz), 65.41, 60.63, 45.10, 44.87, 30.10, 28.14, 22.21, 18.17. HRMS: *m/z* for $C_{26}H_{27}F_4NO_3$ [M + H]$^+$ Calcd.: 478.1927. Found: 478.1931.

*3.1.27. 4-((6-Fluoro-2-(trifluoromethyl)quinolin-4-yl)oxy)butyl 2-(4-isobutylphenyl)propanoate **(8by)***

Colourless oil (87 % yield). IR ($\nu_{max}$/cm$^1$): 3010, 2955, 2880, 1731, 1599, 1577, 1478, 1368. $^1$H NMR (500 MHz, $CDCl_3$) δ: 8.15 (dd, *J* = 9.2, 5.2 Hz, 1H), 7.79 (dd, *J* = 9.2, 2.8 Hz, 1H), 7.61-7.50 (m, 1H), 7.23 (d, *J* = 8.0 Hz, 2H), 7.10 (d, *J* = 8.0 Hz, 2H), 7.01 (s, 1H), 4.28-4.18 (m, 4H), 3.74 (q, *J* = 7.2 Hz, 1H), 2.42 (d, *J* = 7.2 Hz, 2H), 1.95-1.87 (m, 4H), 1.85-1.78 (m, 1H), 1.53 (d, *J* = 7.2 Hz, 3H), 0.88 (d, *J* = 6.6 Hz, 6H). $^{13}$C NMR (125 MHz, $CDCl_3$) δ: 174.73, 162.52 (d, *J* = 5.3 Hz), 161.19 (d, *J* = 250.0 Hz), 148.47 (qd, *J* = 34.4, 2.7 Hz), 145.12, 140.61, 137.78, 132.32 (d, *J* = 9.1 Hz), 129.34, 127.13, 122.60, 121.52 (q, *J* = 34.1 Hz), 121.11 (d, *J* = 25.8 Hz), 105.82 (d, *J* = 23.7 Hz), 97.03 (d, *J* = 1.9 Hz), 68.58, 63.85, 45.20, 44.96, 30.16, 25.35, 25.28, 22.29, 18.33. HRMS: *m/z* for $C_{27}H_{29}F_4NO_3$ [M + H]$^+$ Calcd.: 492.2084. Found: 492.2080.

*3.1.28. 6-((6-Fluoro-2-(trifluoromethyl)quinolin-4-yl)oxy)hexyl 2-(4-isobutylphenyl)propanoate **(8bz)***

Colourless oil (81 % yield). IR ($\nu_{max}$/cm$^1$): 3009, 2951, 2868, 1730, 1599, 1577, 1516, 1375. $^1$H NMR (500 MHz, $CDCl_3$) δ: 8.14 (dd, *J* = 9.2, 5.2 Hz, 1H), 7.82 (dd, *J* = 9.2, 2.8 Hz, 1H), 7.54 (td, *J* = 9.2, 2.8 Hz, 1H), 7.23 (d, *J* = 8.0 Hz, 2H), 7.10 (d, *J* = 8.0 Hz, 2H), 7.04 (s, 1H), 4.22 (t, *J* = 6.4 Hz, 2H), 4.19-4.09 (m, 2H), 3.72 (q, *J* = 7.2 Hz, 1H), 2.44 (d, *J* = 7.2 Hz, 2H), 1.97-1.89 (m, 2H), 1.87-1.80 (m, 1H), 1.72-1.64 (m, 2H), 1.59-1.53 (m, 2H), 1.51 (d, *J* = 7.2 Hz, 3H), 1.46-1.36 (m, 2H), 0.89 (d, *J* = 6.6 Hz, 6H). $^{13}$C NMR (125 MHz, $CDCl_3$) δ: 174.77, 162.68 (d, *J* = 5.2 Hz), 161.16 (d, *J* = 249.9 Hz), 148.49 (qd, *J* = 34.3, 2.6 Hz), 145.12, 140.46, 137.92, 132.29 (d, *J* = 9.1 Hz), 129.27, 127.16, 122.70 (d, *J* = 9.9 Hz), 121.53 (q, *J* = 275.4 Hz), 121.04 (d, *J* = 25.8 Hz), 105.85 (d, *J* = 23.7 Hz), 97.02 (d, *J* = 1.9 Hz), 69.11, 64.37, 45.21, 45.01, 30.17, 28.63, 28.44, 25.57, 25.51, 22.32, 18.42. HRMS: *m/z* for $C_{29}H_{33}F_4NO_3$ [M + H]$^+$ Calcd.: 520.2397. Found: 520.2399.

*3.1.29. 3-((6-Chloro-2-(trifluoromethyl)quinolin-4-yl)oxy)propyl-2-(4-isobutylphenyl)propanoate **(8cx)***

White microcrystals (75 % yield), m.p. 61 °C. IR ($\nu_{max}$/cm$^1$): 3009, 2954, 2900, 1734, 1592, 1502, 1459, 1376. $^1$H NMR (500 MHz, $CDCl_3$) δ: 8.17 (d, *J* = 2.4 Hz, 1H), 8.09 (d, *J* = 9.0 Hz, 1H), 7.73 (dd, *J* = 9.0, 2.4 Hz, 1H), 7.19 (d, *J* = 8.0 Hz, 2H), 7.05 (d, *J* = 8.0 Hz, 2H), 6.95 (s, 1H), 4.46-4.31 (m, 2H), 4.15 (t, *J* = 6.1 Hz, 2H), 3.74 (q, *J* = 7.2 Hz, 1H), 2.40 (d, *J* = 7.2 Hz, 2H), 2.28-2.23 (m, 2H), 1.83-1.77 (m, 1H), 1.52 (d, *J* = 7.2 Hz, 3H), 0.87 (d, *J* = 6.6 Hz, 6H). $^{13}$C NMR (125 MHz, $CDCl_3$) δ: 174.61, 162.03, 149.23 (q, *J* = 34.4 Hz), 146.49, 140.76, 137.61, 133.74, 131.96, 131.27, 129.34, 127.05, 122.31, 121.40 (q, *J* = 275.5 Hz), 121.00, 97.29, 65.57, 60.67, 45.12, 44.89, 30.14, 28.17, 22.28, 18.22. HRMS: *m/z* for $C_{26}H_{27}ClF_3NO_3$ [M + H]$^+$ Calcd.: 494.1632. Found: 494.1633.

*3.1.30. 4-((6-Chloro-2-(trifluoromethyl)quinolin-4-yl)oxy)butyl 2-(4-isobutylphenyl)propanoate **(8cy)***

Colourless oil (77 % yield). IR ($\nu_{max}$/cm$^1$): 3015, 2956, 2891, 1733, 1575, 1509, 1374. $^1$H NMR (500 MHz, $CDCl_3$) δ: 8.18 (d, *J* = 2.4 Hz, 1H), 8.09 (d, *J* = 9.0 Hz, 1H), 7.73 (dd, *J* = 9.0, 2.4 Hz, 1H), 7.23 (d, *J* = 8.0 Hz, 2H), 7.10 (d, *J* = 8.0 Hz, 2H), 7.01 (s, 1H), 4.28-4.18 (m, 4H), 3.74 (q, *J* = 7.2 Hz, 1H), 2.42 (d, *J* = 7.2 Hz, 2H), 2.00-1.86 (m, 4H), 1.85-1.75 (m, 1H), 1.53 (d, *J* = 7.2 Hz, 3H), 0.88 (d, *J* = 6.6 Hz, 6H). $^{13}$C NMR (125 MHz, $CDCl_3$) δ: 174.75, 162.22, 149.32 (q, *J* = 34.5 Hz), 146.52, 140.64, 137.75, 133.67, 131.93, 131.32, 129.34, 127.12, 122.41, 121.40 (q, *J* = 275.6 Hz), 121.05, 97.36, 68.68, 63.82, 45.21, 44.97, 30.17, 25.34, 25.26, 22.30, 18.34. HRMS: *m/z* for $C_{27}H_{29}ClF_3NO_3$ [M + H]$^+$ Calcd.: 508.1788. Found: 508.1791.

*3.1.31. 6-((6-Chloro-2-(trifluoromethyl)quinolin-4-yl)oxy)hexyl 2-(4-isobutylphenyl)propanoate **(8cz)***

Colourless oil (80 % yield). IR ($\nu_{max}$/cm$^1$): 3004, 2952, 2890, 1731, 1591, 1570, 1501, 1459. $^1$H NMR (500 MHz, $CDCl_3$) δ: 8.20 (d, *J* = 2.4 Hz, 1H), 8.08 (d, *J* = 9.0 Hz, 1H), 7.72 (dd, *J* = 9.0, 2.4 Hz, 1H), 7.23 (d, *J* = 8.0 Hz, 2H), 7.10 (d, *J* = 8.0 Hz, 2H), 7.04 (s, 1H), 4.22 (t, *J* = 6.4 Hz, 2H), 4.17-4.09 (m, 2H), 3.72 (q, *J* = 7.2 Hz, 1H), 2.44 (d, *J* = 7.2 Hz, 2H), 1.99-1.90 (m, 2H), 1.91-1.79 (m, 1H), 1.74-1.64 (m, 2H), 1.60-1.54 (m, 2H), 1.52 (d, *J* = 7.2 Hz, 3H), 1.45-1.36 (m, 2H), 0.90 (d, *J* = 6.6 Hz, 6H). $^{13}$C NMR (125 MHz, $CDCl_3$) δ: 174.78, 162.37, 149.31 (q, *J* = 34.3 Hz), 146.49, 140.48, 137.91, 133.57, 131.84, 131.26, 129.27, 127.16, 122.46, 121.44 (q, *J* = 275.6 Hz), 121.08, 97.33, 69.23, 64.39, 45.21, 45.01, 30.18, 28.62, 28.44, 25.58, 25.52, 22.34, 18.44. HRMS: *m/z* for $C_{29}H_{33}ClF_3NO_3$ [M + H]$^+$ Calcd.: 536.2101. Found: 536.2098.

*3.1.32. 3-((6-Methyl-2-(trifluoromethyl)quinolin-4-yl)oxy)propyl-2-(4-isobutylphenyl)propanoate **(8dx)***

White microcrystals (82 % yield), m.p. 69 °C. IR ($\nu_{max}$/cm$^1$): 3013, 2956, 2890, 1733, 1590, 1575, 1412, 1374. $^1$H NMR (500 MHz, $CDCl_3$) δ: 8.05 (d, *J* = 8.6 Hz, 1H), 7.96 (s, 1H), 7.62 (dd, *J* = 8.6, 1.7 Hz, 1H), 7.19 (d, *J* = 8.0 Hz, 2H), 7.05 (d, *J* = 8.0 Hz, 2H), 6.92 (s, 1H), 4.47-4.43 (m, 2H), 4.16-4.13 (m, 2H), 3.74 (q, *J* = 7.2 Hz, 1H), 2.58 (s, 3H), 2.41 (d, *J* = 7.2 Hz, 2H), 2.28-2.23 (m, 2H), 1.83-1.77 (m, 1H), 1.52 (d, *J* = 7.2 Hz, 3H), 0.87 (d, *J* = 6.6 Hz, 6H). $^{13}$C NMR (125 MHz, $CDCl_3$) δ: 174.65, 162.25, 148.04 (q, *J* = 34.0 Hz), 146.68, 140.73, 137.80, 137.63, 133.16, 129.35, 129.33, 127.05, 121.69 (q, *J* = 275.5 Hz), 121.53, 120.59, 96.55, 65.11, 60.82, 45.13, 44.90, 30.13, 28.21, 22.29, 21.84, 18.23. HRMS: *m/z* for $C_{27}H_{30}F_3NO_3$ [M + H]$^+$ Calcd.: 474.2178. Found: 474.2171.

*3.1.33. 4-((6-Methyl-2-(trifluoromethyl)quinolin-4-yl)oxy)butyl 2-(4-isobutylphenyl)propanoate **(8dy)***

Colourless oil (89 % yield). IR ($\nu_{max}$/cm$^1$): 3016, 2954, 2891, 1731, 1591, 1575, 1411, 1366. $^1$H NMR (500 MHz, $CDCl_3$) δ: 8.06 (d, *J* = 8.6 Hz, 1H), 7.98 (s, 1H), 7.63 (dd, *J* = 8.6, 1.8 Hz, 1H), 7.23 (d, *J* = 8.0 Hz, 2H), 7.10 (d, *J* = 8.0 Hz, 2H), 6.97 (s, 1H), 4.30-4.22 (m, 2H), 4.22-4.17 (m, 2H), 3.73 (q, *J* = 7.2 Hz, 1H), 2.59 (s, 3H), 2.43 (d, *J* = 7.2 Hz, 2H), 1.99-1.87 (m, 4H), 1.87-1.77 (m, 1H), 1.53 (d, *J* = 7.2 Hz, 3H), 0.88 (d, *J* = 6.6 Hz, 6H). $^{13}$C NMR (125 MHz, $CDCl_3$) δ: 174.75, 162.43, 148.12 (q, *J* = 34.0 Hz), 146.70, 140.61, 137.78, 137.73, 133.12, 129.38, 129.34, 127.12, 121.69 (q, *J* = 275.5 Hz), 121.62, 120.62, 96.60, 68.33, 63.98, 45.21, 44.98, 30.16, 25.41, 25.36, 22.31, 21.86, 18.37. HRMS: *m/z* for $C_{28}H_{32}F_3NO_3$ [M + H]$^+$ Calcd.: 488.2334. Found: 488.2335.

*3.1.34. 6-((6-Methyl-2-(trifluoromethyl)quinolin-4-yl)oxy)hexyl 2-(4-isobutylphenyl)propanoate **(8dz)***

Colourless oil (91 % yield). IR ($\nu_{max}$/cm$^1$): 3011, 2952, 2887, 1728, 1592, 1575, 1509, 1412. $^1$H NMR (500 MHz, $CDCl_3$) δ: 8.05 (d, *J* = 8.6 Hz, 1H), 8.01 (s, 1H), 7.62 (dd, *J* = 8.6, 1.8 Hz, 1H), 7.23 (d, *J* = 8.0 Hz, 2H), 7.10 (d, *J* = 8.0 Hz, 2H), 7.00 (s, 1H), 4.21 (t, *J* = 6.4 Hz, 2H), 4.19-4.09 (m, 2H), 3.72 (q, *J* = 7.2 Hz, 1H), 2.59 (s, 3H), 2.44 (d, *J* = 7.2 Hz, 2H), 2.00-1.90 (m, 2H), 1.90-1.80 (m, 1H), 1.74-1.64 (m, 2H), 1.62-1.53 (m, 2H), 1.52 (d, *J* = 7.2 Hz, 3H), 1.47-1.36 (m, 2H), 0.90 (d, *J* = 6.6 Hz, 6H). $^{13}$C NMR (125 MHz, $CDCl_3$) δ: 174.79, 162.60, 148.14 (q, *J* = 34.0 Hz), 146.70, 140.48, 137.91, 137.66, 133.07, 129.36, 129.28, 127.15, 121.73 (q, *J* = 275.4 Hz), 121.69, 120.68, 96.60, 68.83, 64.43, 45.22, 45.01, 30.18, 28.69, 28.44, 25.61, 25.52, 22.34, 21.85, 18.44. HRMS: *m/z* for $C_{30}H_{36}F_3NO_3$ [M + H]$^+$ Calcd.: 516.2647. Found: 516.2644.

*3.1.35. 6-(4-Oxo-2-(trifluoromethyl)quinolin-1(4H)-yl)hexyl 2-(4-isobutylphenyl)propanoate **(9az)***

Colourless oil (69 % yield). IR ($\nu_{max}$/cm$^1$): 3008, 2955, 2896, 1731, 1620, 1573, 1459. $^1$H NMR (500 MHz, $CDCl_3$) δ: 8.03 (d, *J* = 8.4 Hz, 1H), 7.94 (d, *J* = 8.4 Hz, 1H), 7.75-7.67 (m, 1H), 7.53-7.46 (m, 1H),

7.26 (s, 1H), 7.23 (d, *J* = 8.1 Hz, 2H), 7.11 (d, *J* = 8.1 Hz, 2H), 4.49 (t, *J* = 6.6 Hz, 2H), 4.11 (td, *J* = 6.6, 3.3 Hz, 2H), 3.71 (q, *J* = 7.2 Hz, 1H), 2.45 (d, *J* = 7.2 Hz, 2H), 1.89-1.75 (m, 3H), 1.72-1.60 (m, 2H), 1.51 (d, *J* = 7.2 Hz, 3H), 1.49-1.45 (m, 2H), 1.41-1.34 (m, 2H), 0.90 (d, *J* = 6.6 Hz, 6H). $^{13}$C NMR (125 MHz, $CDCl_3$) δ: 174.83, 161.06, 147.65, 140.48, 137.90, 137.01 (q, *J* = 31.7 Hz), 130.29, 129.28, 128.07, 127.16, 125.17, 124.05, 123.12 (q, *J* = 274.5 Hz), 119.71, 111.75 (q, *J* = 5.7 Hz), 66.38, 64.59, 45.22, 45.02, 30.17, 28.70, 28.48, 25.65, 25.57, 22.36, 18.43. HRMS: *m/z* for $C_{29}H_{34}F_3NO_3$ [M + H]$^+$ Calcd.: 502.2491. Found: 502.2488.

#### *3.1.36. 6-(6-Methyl-4-oxo-2-(trifluoromethyl)quinolin-1(4H)-yl)hexyl-2-(4-isobutylphenyl)propanoate **(9dz)***

Colourless oil (72 % yield). IR ($\nu_{max}$/cm$^1$): 3013, 2997, 2885, 1733, 1622, 1575, 1436. $^1$H NMR (500 MHz, $CDCl_3$) δ: 7.84 (d, *J* = 8.5 Hz, 1H), 7.78 (s, 1H), 7.55 (dd, *J* = 8.5, 1.7 Hz, 1H), 7.23 (d, *J* = 8.1 Hz, 2H), 7.22 (s, 1H), 7.10 (d, *J* = 8.1 Hz, 2H), 4.46 (t, *J* = 6.6 Hz, 2H), 4.11 (td, *J* = 6.6, 2.9 Hz, 2H), 3.71 (q, *J* = 7.2 Hz, 1H), 2.55 (s, 3H), 2.45 (d, *J* = 7.2 Hz, 2H), 1.90-1.83 (m, 1H), 1.83-1.77 (m, 2H), 1.71-1.60 (m, 2H), 1.51 (d, *J* = 7.2 Hz, 3H), 1.49-1.43 (m, 2H), 1.42-1.33 (m, 2H), 0.90 (d, *J* = 6.6 Hz, 6H). $^{13}$C NMR (125 MHz, $CDCl_3$) δ: 174.80, 160.59, 145.93, 140.48, 137.90, 136.46 (q, *J* = 31.6 Hz), 135.02, 132.34, 129.28, 127.71, 127.16, 123.18 (q, *J* = 275.6 Hz), 123.15, 119.67, 111.51, 66.33, 64.60, 45.23, 45.03, 30.18, 28.73, 28.49, 25.66, 25.58, 22.36, 21.70, 18.43. HRMS: *m/z* for $C_{30}H_{36}F_3NO_3$ [M + H]$^+$ Calcd.: 516.2647. Found: 516.2642.

### *3.2. X-ray, biological and computational studies*

Details of the experimental techniques utilized for X-ray, biological and computational studies are mentioned in the supplementary file.

## Declaration of Competing Interest

The authors declare that they have no known competing financial interests or personal relationships that could have appeared to influence the work reported in this paper.

## Acknowledgments

The Deanship of Scientific Research (DSR) at King Abdulaziz University, Jeddah, Saudi Arabia has funded this project under grant No. RG-17-166-42. The authors, therefore, gratefully acknowledge DSR technical and financial support.

## Appendix A. Supplementary material

Supplementary data to this article can be found online at

## References

[1] J. Naesdal, K. Brown, NSAID-associated adverse effects and acid control aids to prevent them: a review of current treatment options, Drug Saf. 29 (2) (2006) 119-132, https://doi.org/10.2165/00002018-200629020-00002.

[2] J.-M. Dogné, C.T. Supuran, D. Pratico, Adverse cardiovascular effects of the coxibs, J. Med. Chem. 48 (7) (2005) 2251-2257, https://doi.org/10.1021/jm0402059.

[3] T. Costa, E. Fernandez-Villalba, V. Izura, A.M. Lucas-Ochoa, N.J. Menezes-Filho, R. C. Santana, M.D. de Oliveira, F.M. Araújo, C. Estrada, V. Silva, S.L. Costa, M. T. Herrero, Combined 1-deoxynojirimycin and ibuprofen treatment decreases microglial activation, phagocytosis and dopaminergic degeneration in MPTP-treated mice, J. Neuroimmune Pharmacol. 16 (2) (2021) 390-402, https://doi.org/10.1007/s11481-020-09925-8.

[4] T. Behl, I. Kaur, O. Fratila, R. Brata, S. Bungau, Exploring the potential of therapeutic agents targeted towards mitigating the events associated with amyloid-β cascade in Alzheimer's disease, Int. J. Mol. Sci. 21 (2020) 1-24, https://doi.org/10.3390/ijms21207443.

[5] L.S. Mendonça, C. Nóbrega, S. Tavino, M. Brinkhaus, C. Matos, S. Tomé, R. Moreira, D. Henriques, B.K. Kaspar, L.P. De Almeida, Ibuprofen enhances synaptic function and neural progenitors proliferation markers and improves neuropathology and motor coordination in Machado - Joseph disease models, Hum. Mol. Genet. 28 (2019) 3691-3703, https://doi.org/10.1093/hmg/ddz097.

[6] S. Bua, L. Lucarini, L. Micheli, M. Menicatti, G. Bartolucci, S. Selleri, L. Di, C. Mannelli, C. Ghelardini, E. Masini, F. Carta, P. Gratteri, A. Nocentini, C. T. Supuran, Bioisosteric development of multitarget nonsteroidal anti- infl ammatory drug carbonic anhydrases inhibitor hybrids for the management of rheumatoid arthritis, J. Med. Chem. 63 (2020) 2325-2342, https://doi.org/10.1021/acs.jmedchem.9b01130.

[7] S. Bua, L. Di Cesare Mannelli, D. Vullo, C. Ghelardini, G. Bartolucci, A. Scozzafava, C.T. Supuran, F. Carta, Design and synthesis of novel nonsteroidal anti-inflammatory drugs and carbonic anhydrase inhibitors hybrids (NSAIDs-CAIs) for the treatment of rheumatoid arthritis, J. Med. Chem. 60 (2017) 1159-1170, doi: 10.1021/acs.jmedchem.6b01607.

[8] A.Z. Abdel-azeem, A.A. Abdel-hafez, G.S. El-karamany, H.H. Farag, Chlorzoxazone esters of some non-steroidal anti-inflammatory (NSAI) carboxylic acids as mutual prodrugs: design, synthesis, pharmacological investigations and docking studies, Bioorg. Med. Chem. 17 (2009) 3665-3670, https://doi.org/10.1016/j.bmc.2009.03.065.

[9] V.K. Redasani, S.B. Bari, Synthesis and evaluation of mutual prodrugs of ibuprofen with menthol, thymol and eugenol, Eur. J. Med. Chem. 56 (2012) 134-138, https://doi.org/10.1016/j.ejmech.2012.08.030.

[10] A. Sakr, S Rezq, S.M. Ibrahim, E. Soliman, M.M. Baraka, D.G. Romero, H. Kothayer, Design and synthesis of novel quinazolinones conjugated ibuprofen, indole acetamide, or thioacetohydrazide as selective COX-2 inhibitors: anti-inflammatory, analgesic, and anticancer activities, J. Enzyme Inhib. Med. Chem. 36 (2021) 1810-1828.

[11] I. Chaaban, O.H. Rizk, T.M. Ibrahim, S.S. Henen, E.S.M. El-Khawass, A.E. Bayad, I. M. El-Ashmawy, H.A. Nematalla, Synthesis, anti-inflammatory screening, molecular docking, and COX-1,2/-5-LOX inhibition profile of some novel quinoline derivatives, Bioorg. Chem. 78 (2018) 220-235, https://doi.org/10.1016/j.bioorg.2018.03.023.

[12] Z.-H. Huang, L.-Q. Yin, L.-P. Guan, Z.-H. Li, C. Tan, Screening of chalcone analogs with anti-depressant, anti-inflammatory, analgesic, and COX-2-inhibiting effects, Bioorg. Med. Chem. Lett. 30 (11) (2020) 127173, https://doi.org/10.1016/j.bmcl.2020.127173.

[13] M. Mroueh, W.H. Faour, W.N. Shebaby, C.F. Daher, T.M. Ibrahim, H.M. Ragab, Synthesis, biological evaluation and modeling of hybrids from tetrahydro-1H-pyrazolo[3,4-b]quinolines as dual cholinestrase and COX-2 inhibitors, Bioorg. Chem. 100 (2020) 103895, https://doi.org/10.1016/j.bioorg.2020.103895.

[14] S.A.H. El-Feky, Z.K. Abd El-Samii, N.A. Osman, J. Lashine, M.A. Kamel, H. K. Thabet, Synthesis, molecular docking and anti-inflammatory screening of novel quinoline incorporated pyrazole derivatives using the Pfitzinger reaction II, Bioorg. Chem. 58 (2015) 104-116, https://doi.org/10.1016/j.bioorg.2014.12.003.

[15] R. Ghodsi, A. Zarghi, B. Daraei, M. Hedayati, Design, synthesis and biological evaluation of new 2,3-diarylquinoline derivatives as selective cyclooxygenase-2 inhibitors, Bioorg. Med. Chem. 18 (3) (2010) 1029-1033, https://doi.org/10.1016/j.bmc.2009.12.060.

[16] M.H. Abdelrahman, B.G.M. Youssif, M.A. abdelgawad, A.H. Abdelazeem, H. M. Ibrahim, A.E.G.A. Moustafa, L. Treamblu, S.N.A. Bukhari, Synthesis, biological evaluation, docking study and ulcerogenicity profiling of some novel quinoline-2-carboxamides as dual COXs/LOX inhibitors endowed with anti-inflammatory activity, Eur. J. Med. Chem. 127 (2017) 972-985, https://doi.org/10.1016/j.ejmech.2016.11.006.

[17] C. Tseng, C. Tung, S. Peng, Y. Chen, C. Tzeng, C. Cheng, Discovery of pyrazolo[4,3-c]quinolines derivativesas potential anti-inflammatory agents through inhibiting of NO production, Molecules 23 (2018) 1036, https://doi.org/10.3390/molecules23051036.

[18] U. Debnath, S. Mukherjee, N. Joardar, S.P. Sinha Babu, K. Jana, A.K. Misra, Aryl quinolinyl hydrazone derivatives as anti-inflammatory agents that inhibit TLR4 activation in the macrophages, Eur. J. Pharm. Sci. 134 (2019) 102-115, https://doi.org/10.1016/j.ejps.2019.04.016.

[19] D.N. Deaton, Y. Do, J. Holt, M.R. Jeune, H.F. Kramer, A.L. Larkin, L.A. Orband-Miller, G.E. Peckham, C. Poole, D.J. Price, L.T. Schaller, Y. Shen, L.M. Shewchuk, E. L. Stewart, J.D. Stuart, S.A. Thomson, P. Ward, J.W. Wilson, T. Xu, J.H. Guss, C. Musetti, A.R. Rendina, K. Affleck, D. Anders, A.P. Hancock, H. Hobbs, S. T. Hodgson, J. Hutchinson, M.V. Leveridge, H. Nicholls, I.E.D. Smith, D.O. Somers, H.F. Sneddon, S. Uddin, A. Cleasby, P.N. Mortenson, C. Richardson, G. Saxty, The discovery of quinoline-3-carboxamides as hematopoietic prostaglandin D synthase (H-PGDS) inhibitors, Bioorg. Med. Chem. 27 (8) (2019) 1456-1478, https://doi.org/10.1016/j.bmc.2019.02.017.

[20] T.A. Rano, E. Sieber-McMaster, P.D. Pelton, M. Yang, K.T. Demarest, G.-H. Kuo, Design and synthesis of potent inhibitors of cholesteryl ester transfer protein (CETP) exploiting a 1, 2, 3, 4-tetrahydroquinoline platform, Bioorg. Med. Chem. Lett. 19 (9) (2009) 2456-2460, https://doi.org/10.1016/j.bmcl.2009.03.051.

[21] R.C. Bernotas, D.H. Kaufman, R.R. Singhaus, J. Ullrich, R. Unwalla, E. Quinet, P. Nambi, A. Wilhelmsson, A. Goos-Nilsson, J. Wrobel, 4- (3-Aryloxyaryl) quinoline alcohols are liver X receptor agonists, Bioorg. Med. Chem. 17 (23) (2009) 8086-8092, https://doi.org/10.1016/j.bmc.2009.10.001.

[22] B. Hu, J. Jetter, D. Kaufman, R. Singhaus, R. Bernotas, R. Unwalla, E. Quinet, D. Savio, A. Halpern, M. Basso, J. Keith, V. Clerin, L. Chen, Q.-Y. Liu, I. Feingold, C. Huselton, F. Azam, A. Goos-Nilsson, A. Wilhelmsson, P. Nambi, J. Wrobel, Further modification on phenyl acetic acid based quinolines as liver X receptor modulators, Bioorg. Med. Chem. 15 (10) (2007) 3321-3333, https://doi.org/10.1016/j.bmc.2007.03.013.

[23] N.A. Sharif, P. Katoli, D. Scott, L. Li, C. Kelly, S. Xu, S. Husain, C. Toris, C. Crosson, FR-190997, a nonpeptide bradykinin B2 -receptor PartialAgonist, is a potent and

efficacious intraocular pressure lowering agent in ocular hypertensive cynomolgus monkeys, Drug Dev. Res. 75 (4) (2014) 211-223, https://doi.org/10.1002/ddr.2014.75.issue-410.1002/ddr.21174.
[24] A.D. Tiwari, S.S. Panda, A.S. Girgis, S. Sahu, R.F. George, A.M. Srour, B. La Starza, A.M. Asiri, C.D. Hall, A.R. Katritzky, Microwave assisted synthesis and QSAR study of novel NSAID acetaminophen conjugates with amino acid linkers, Org. Biomol. Chem. 12 (2014) 7238-7249, https://doi.org/10.1039/c4ob01281j.
[25] S.S. Panda, A.S. Girgis, H.H. Honkanadavar, R.F. George, A.M. Srour, Synthesis of new ibuprofen hybrid conjugates as potential anti-inflammatory and analgesic agents, Future Med. Chem. 12 (15) (2020) 1369-1386, https://doi.org/10.4155/fmc-2020-0109.
[26] D.Y. Li, M.Y. Xue, Z.R. Geng, P.Y. Chen, The suppressive effects of Bursopentine (BP5) on oxidative stress and NF-κB activation in lipopolysaccharide-activated murine peritoneal macrophages, Cell. Physiol. Biochem. 29 (2012) 9-20, https://doi.org/10.1159/000337581.
[27] W. Wang, P. Liu, C. Hao, L. Wu, W. Wan, X. Mao, Neoagaro-oligosaccharide monomers inhibit inflammation in LPS-stimulated macrophages through suppression of MAPK and NF-κB pathways, Sci. Rep. 7 (2017) 44252, https://doi.org/10.1038/srep44252.
[28] K.-N. Kim, S.-J. Heo, W.-J. Yoon, S.-M. Kang, G. Ahn, T.-H. Yi, Y.-J. Jeon, Fucoxanthin inhibits the inflammatory response by suppressing the activation of NF-kappaB and MAPKs in lipopolysaccharide-induced RAW264.7 macrophages, Eur. J. Pharmacology 649 (2010) 369-375, https://doi.org/10.1016/j.ejphar.2010.09.032.
[29] M.-S. Yoo, J.-S. Shin, H.-E. Choi, Y.-W. Cho, M.-H. Bang, N.-I. Baek, K.-T. Lee, Fucosterol isolated from *Undaria pinnatifida* inhibits lipopolysaccharide-induced production of nitric oxide and pro-inflammatory cytokines via the inactivation of nuclear factor-κB and p38 mitogen-activated protein kinase in RAW264.7 macrophages, Food Chemistry 135 (2012) 967-975. doi. 10.1016/j.foodchem.2012.05.039.
[30] E.T. da Silva, G.F. de Andrade, A.d.S. Araújo, M.C.S. Lourenço, M.V.N. de Souza, Antibacterial activity of new substituted 4-N-alkylated-2-trifluoromethyl-quinoline analogues against sensitive and resistant Mycobacterium tuberculosis strains, Eur. J. Pharm. Sci. 157 (2021) 105596, https://doi.org/10.1016/j.ejps.2020.105596.
[31] S. Maračić, S.D. Lapić, T. Opačak-Bernardi, L. Glavaš-Obrovac, V. Vrček, S. Raić-Malić, Quinoline and ferrocene conjugates: synthesis, computational study and biological evaluations, Appl. Organomet. Chem. 33 (2019), e4628, https://doi.org/10.1002/aoc.4628.
[32] S.S. Panda, S.C. Jain, New trifluoromethyl quinolone derivatives: synthesis and investigation of antimicrobial properties, Bioorg. Med. Chem. Lett. 23 (11) (2013) 3225-3229, https://doi.org/10.1016/j.bmcl.2013.03.120.
[33] A.N. Hajhussein, L.S. Abuzahra, A. Pietrzak, M.F. Sadek, M.O. Ali, J. Wojciechowski, A.C. Friedli, P. Kaszynski, Synthesis of 4-alkoxypyridines as intermediates for zwitterionic liquid crystals, Arkivoc (2018) 225-235, https://doi. org/10.24820/ark.5550190.p010.700.
[34] S.S. Panda, A.S. Girgis, S.J. Thomas, J.E. Capito, R.F. George, A. Salman, M.A. El-Manawaty, A. Samir, Synthesis, pharmacological profile and 2D-QSAR studies of curcumin-amino acid conjugates as potential drug candidates, Eur. J. Med. Chem. 196 (2020), 112293, https://doi.org/10.1016/j.ejmech.2020.112293.
[35] A. Zarghi, S. Arfaei, Selective COX-2 inhibitors: a review of their structure-activity relationships, Iran. J. Pharm. Res. 10 (2011) 655-683.
[36] J.R. Caso, J.M. Pradillo, O. Hurtado, P. Lorenzo, M.A. Moro, I. Lizasoain, Toll-like receptor 4 is involved in brain damage and inflammation after experimental stroke, Circulation 115 (12) (2007) 1599-1608, https://doi.org/10.1161/CIRCULATIONAHA.106.603431.
[37] Availablr from <http://www.premierbiosoft.com/tech_notes/PCR_Primer_Design.html>.
[38] A.S. Girgis, S.R. Tala, P.V. Oliferenko, A.A. Oliferenko, A.R. Katritzky, Computer-assisted rational design, synthesis, and bioassay of nonsteroidal anti-inflammatory agents, Eur. J. Med. Chem. 50 (2012) 1-8, https://doi.org/10.1016/j.ejmech.2011.11.034.
[39] M.N. Aziz, S.S. Panda, E.M. Shalaby, N.G. Fawzy, A.S. Girgis, Facile synthetic approach towards vasorelaxant active 4-hydroxyquinazoline-4-carboxamides, RSC Adv. 9 (49) (2019) 28534-28540, https://doi.org/10.1039/C9RA04321G.
[40] Available from: <http://www.codessa-pro.com/manuals/manual.htm>.